NATIONAL ADVISORY COMMITTEE FOR AERONAUTICS

TECHNICAL NOTE 2405

INVESTIGATION OF NACA 64,2-432 AND 64,3-440 AIRFOIL SECTIONS WITH BOUNDARY-LAYER CONTROL AND AN ANALYTICAL STUDY OF THEIR POSSIBLE APPLICATIONS

By Elmer A. Horton, Stanley F. Racisz,
and Nicholas J. Paradiso

Langley Aeronautical Laboratory
Langley Field, Va.

Washington
July 1951

NATIONAL ADVISORY COMMITTEE FOR AERONAUTICS

TECHNICAL NOTE 2405

INVESTIGATION OF NACA 64,2-432 AND 64,3-440 AIRFOIL SECTIONS WITH BOUNDARY-LAYER CONTROL AND AN ANALYTICAL STUDY OF THEIR POSSIBLE APPLICATIONS

By Elmer A. Horton, Stanley F. Racisz, and Nicholas J. Paradiso

SUMMARY

NACA 64-series airfoil sections of 32- and 40-percent-chord thickness ratio have been derived and an investigation was made to determine the effect of boundary-layer control by means of suction through a slot at 0.60 airfoil chord on the pressure distribution, lift, and drag characteristics of the NACA 64,2-432 and 64,3-440 airfoil sections. The effect on the section aerodynamic characteristics of boundary-layer control by means of a slot at 0.50 airfoil chord and by means of area suction from 0.55 airfoil chord to 0.71 airfoil chord was also investigated for the NACA 64,3-440 airfoil. An analysis was made to determine whether the maximum lift-drag ratio and the aspect ratio for maximum lift-drag ratio could be increased by the use of thick airfoils and boundary-layer control on structurally feasible wings. The section data presented and employed in the analysis were obtained with standard roughness applied to the leading edges of the models. This roughness was probably more severe than that likely to be encountered on practical aircraft under normal operating conditions; therefore, the drag coefficients measured both with and without boundary-layer control may be somewhat high as compared with practical flight values.

The results indicate that substantial reductions in the wake drag were obtained through a wide range of lift coefficient with relatively moderate flow coefficients and pressure-loss coefficients. The minimum total-drag coefficients (including the drag coefficients of the suction power) for the 32- and 40-percent-thick sections in the rough surface condition were 0.017 and 0.028, respectively. With the results obtained for the 32- and 40-percent-thick sections together with the data which are available in the literature the characteristics of a number of hypothetical wings were calculated. These calculations indicate that, by the use of boundary-layer control, the maximum obtainable lift-drag ratio of structurally feasible wings may be increased by as much as 13 percent for the wing alone and as much as 20 percent for the wing with a parasite drag coefficient of 0.015 added. The calculations were made from section data for the rough-leading-edge condition; therefore,

the possible gains indicated do not depend on the attainment of extensive laminar layers.

INTRODUCTION

The use of wings of high aspect ratio with resulting low induced drag coefficients would appear to be one means of increasing the lift-drag ratio of an airplane. For structural reasons, however, the root section must increase in thickness ratio with aspect ratio and, for root-section thickness ratios in excess of some critical value, the profile drag increases more rapidly with aspect ratio than the induced drag decreases; thus, the maximum lift-drag ratio obtainable by this means is limited. For example, reference 1 shows that, for wings having a ratio of root chord to tip chord of 2.5 and a ratio of span to root thickness of 35, increasing the aspect ratio beyond 12 results in a decrease in the maximum lift-drag ratio due to the increased profile drag of the thick root sections. The large drags of the thick airfoil sections are primarily a result of separation of the turbulent boundary layer from the rearward parts of the airfoil.

Boundary-layer control by means of a single midchord suction slot has been found to be quite effective in delaying trailing-edge separation and thereby increasing the maximum lift coefficient and decreasing the drag coefficient of many airfoil sections. (See, for example, references 2 to 7.) For this reason, it was believed that, by the use of airfoils of 32- to 40-percent chord in thickness together with boundary-layer control, some of the improvements in lift-drag ratio associated with high aspect ratios might be realized on structurally feasible wings. Airfoil sections of 32- and 40-percent-chord thickness ratio were accordingly derived and models of these sections were built and tested with and without boundary-layer control in the Langley two-dimensional low-turbulence tunnels to obtain the lift and drag characteristics. Most of the tests were made with standard leading-edge roughness applied to the surfaces of the models. This roughness was probably more severe than that likely to be encountered on practical aircraft under normal operating conditions; therefore, the drag coefficients measured both with and without boundary-layer control may be somewhat high as compared with practical flight values. However, the results obtained for the rough-leading-edge condition are believed to be more nearly comparable with practical flight values than are results obtained for the aerodynamically smooth condition.

The results of the wind-tunnel investigation of these models are presented and, together with the data presented in references 2 to 7, are analyzed to determine the effect of boundary-layer control and increased aspect ratio on the lift-drag ratio of a series of structurally similar wings of various taper ratios.

SYMBOLS

c_l	section lift coefficient $(l/q_o c)$
l	section lift, pounds
c	airfoil chord, feet
q	dynamic pressure, pounds per square foot $(\rho V^2/2)$
V	velocity, feet per second
v	local velocity, feet per second
ρ	mass density, slugs per cubic foot
R	free-stream Reynolds number based on airfoil chord
c_d	section profile-drag coefficient $(d/q_o c)$
d	section drag, pounds
c_{d_b}	equivalent blower section drag coefficient $(C_Q C_P)$
c_{d_T}	section total-drag coefficient $\left(c_d + \frac{\eta_p}{\eta_b} c_{d_b}\right)$
C_Q	flow coefficient $(Q/V_o cs)$
Q	volume rate of flow, cubic feet per second
s	span of boundary-layer control slot or porous material, feet
C_P	pressure-loss coefficient $\left(\frac{H_o - H_b}{q_o}\right)$
H	total pressure, pounds per square foot
η_p	efficiency of main propulsive unit
η_b	efficiency of boundary-layer-control blower and ducts
A	aspect ratio (b^2/S_W)
S_W	wing area, square feet
Δv_a	increment of local velocity caused by additional type of load distribution, feet per second

b	wing span
L	wing lift, pounds
D	wing drag, pounds
L/D	wing lift-drag ratio
α_o	section angle of attack, degrees
λ	taper ratio (c_t/c_r)
x	distance along chord from leading edge, feet
y	perpendicular distance above chord, feet
S	pressure coefficient $\left(\frac{H_o - p}{q_o}\right)$
p	local static pressure, pounds per square foot

Subscripts:

max	maximum conditions
b	duct conditions
o	free-stream conditions
t	wing tip
r	wing root

DERIVATION OF AIRFOIL SECTIONS

The first attempt to derive 64-series airfoils of 32- and 40-percent thickness consisted merely in a linear scaling of the same ψ and ϵ values employed in reference 8 to derive the related 64-series sections of different thickness ratio. The resultant airfoils were found, however, to have extremely high values of the peak negative pressure coefficient on the basic thickness form at zero lift. The ψ and ϵ values were, therefore, modified to reduce the negative pressure coefficient and thus to increase the critical speed. The theoretical pressure distributions and ordinates for the resultant airfoils, designated NACA 64,2-032 and NACA 64,3-040, are given in figures 1 and 2.

Both airfoil sections were cambered to have design lift coefficients of 0.4. The conventional $a = 1.0$ mean line (reference 8) was employed in cambering the NACA 64,2-032 airfoil section. Because of the large slope of the mean line near the leading edge and the magnitude of the ordinates of the symmetrical airfoil near the leading edge, however, the resultant cambered section appeared to have a flat spot at the leading edge. For this reason, the 40-percent-thick section was cambered with an $a = 1.0$ mean line which was modified near the leading edge so that the slope would be reduced. The forward 15 percent of the $a = 1.0$ mean line was replaced by a polynomial of the form:

$$y = a_0 + a_1 x + a_2 x^2 + a_3 x^3$$

where the coefficients (a_0, a_1, a_2, and a_3) were determined by the mean-line ordinates at the zero and 15-percent-chord stations and by the first and second derivatives of the $a = 1.0$ mean line at the 15-percent-chord station. The ordinates of the $a = 1.0$ mean line are given by the expression

$$y = -\frac{c_l}{4\pi}\left[(1 - x)\log_e(1 - x) + x \log_e x\right]$$

where c_l is the design lift coefficient. The ordinates for the cambered airfoils which are designated NACA 64,2-432 and NACA 64,3-440, $a = 1.0$ (modified) are given in tables I and II.

APPARATUS AND TESTS

Wind tunnel.- The tests were conducted in the two Langley two-dimensional low-turbulence tunnels. The test sections of the two tunnels are similar and are 3 feet wide and 7.5 feet high. The models completely spanned the 3-foot-wide test section so that two-dimensional flow would be obtained. Lift measurements were made by taking the difference between the integrated pressure reaction upon the floor and ceiling of the tunnel, and profile-drag measurements were obtained from surveys of the momentum defect in the wake. A more complete description of the tunnels and the methods of obtaining and reducing the data are given in reference 9.

Models.- The 2-foot-chord models of the NACA 64,2-432 and 64,3-440 airfoil sections were constructed of chordwise-laminated mahogany according to the ordinates presented in tables I and II, respectively.

A sketch and a photograph of the NACA 64,2-432 airfoil section showing the 0.016c slot at the 0.60c position are shown in figures 3 and 4. The NACA 64,3-440 airfoil section was tested with three separate suction configurations: a single suction slot located at 0.50c (fig. 5), a single suction slot located at 0.60c (fig. 5), and area suction provided by means of a porous material (sintered bronze) on the upper surface extending from 0.55c to 0.71c (fig. 6). The porosity of the sintered-bronze material was such that, with air at standard conditions, a pressure drop of 0.032 pounds per square inch across the material resulted in a velocity of 1.0 foot per second normal to the surface. The flow through the material varied directly with the pressure drop, a condition that is characteristic of flow through dense filters.

The duct within the models (figs. 3 to 6) was connected to the inlet of a variable-speed blower by means of a pipe line containing an orifice meter for measuring flows. Loss of total pressure through the slot or porous material was taken to be the difference between free-stream total pressure and the pressure within the duct measured by a flush-type orifice in the end of the model duct opposite to that from which the air was removed. For the rates of flow involved, the velocities in the duct of the model were sufficiently low so that the pressure thus measured may be assumed equal to the total pressure.

Tests.- The models were first tested, prior to installation of the slot, without boundary-layer control in the aerodynamically smooth condition and with standard leading-edge roughness. The roughness employed consisted of 0.011-inch carborundum grains spread over a surface length of 0.08c back from the leading edge on both upper and lower surfaces of the models. The grains were spread to cover from 5 to 10 percent of the included area.

A review of the available data on boundary-layer control indicated that, in order for a single suction slot to be most effective in reducing the drag, it should be located near the point where separation occurred without boundary-layer control. From experimental pressure-distribution measurements at the design lift coefficient in both the smooth and rough conditions, separation was found to occur on the upper surface at approximately 0.50c on the NACA 64,3-440 airfoil section and 0.60c on the NACA 64,2-432 airfoil section. Both airfoil sections were tested at a Reynolds number of 2.2×10^6 with a suction slot at 0.60c and with flow coefficients ranging from 0 to 0.038. Most of the tests were made with the model in the rough condition, which is believed to be more representative for wings of practical construction. In addition, in order to evaluate the effect on the section lift and drag characteristics of varying amounts of suction together with such variables as slot location, roughness, and area suction or suction through a single slot, the NACA 64,3-440 airfoil section was tested with the following configurations and Reynolds numbers:

(1) In the smooth condition with a suction slot at 0.60c and a Reynolds number of 2.2×10^6

(2) In the rough condition with the slot at 0.50c and a Reynolds number of 3.0×10^6

(3) In the rough condition with a porous upper surface from 0.55c to 0.71c at a Reynolds number of 2.2×10^6

All tests were made for various flow coefficients from 0 to a maximum of 0.020 to 0.025 depending on the configuration. Most of the tests were run at a Reynolds number of 2.2×10^6 and a Mach number of 0.15. The remainder of the tests were run at a Reynolds number of 3.0×10^6 at a pressure of 2 atmospheres absolute and a Mach number of 0.10.

RESULTS AND DISCUSSION

The discussion of the results is presented in two parts. The first part is a discussion of the data obtained from tests of the NACA 64,2-432 and 64,3-440 airfoil sections, and the second part is an evaluation of the effect of boundary-layer control on the aspect ratio for maximum lift-drag ratio and on the maximum lift-drag ratio of several hypothetical wings.

Airfoil-Section Data

Experimental pressure distributions obtained for the two airfoils both with and without boundary-layer control are compared with the theoretical distributions in figures 7 and 8. The basic aerodynamic data, that is, lift, drag, and pressure losses, obtained in the wind-tunnel investigation are presented in coefficient form in figures 9 to 13 for each of the configurations investigated. The section lift and pressure-loss coefficients are presented as functions of the section angle of attack and the drag coefficients as functions of the section lift coefficient.

The drag data obtained for the two airfoil sections are presented as section profile-drag and section total-drag coefficients for all configurations. The section profile-drag coefficient as determined by measuring the momentum defect in the wake indicates the effectiveness of boundary-layer control in reducing the external drag; it does not, however, provide an adequate means of judging the over-all effectiveness of boundary-layer control because no account is taken of the boundary-layer-control suction power. For this reason, the total drag, which is

the sum of the wake drag and the drag equivalent of the suction power (C_pC_Q), is also given. This method of accounting for the suction power has been shown to be valid (reference 6) if the efficiency of the boundary-layer control system is the same as the efficiency of the main propulsive system.

Pressure distribution.- The theoretical and experimental pressure distributions for the NACA 64,2-432 and 64,3-440 airfoil sections at angles of attack of 0° and 4°, respectively, are presented in figures 7 and 8. The data presented show that, for the smooth condition without boundary-layer control, there is very little separation on the upper surface of the NACA 64,2-432 airfoil section and that the experimental and theoretical pressure distributions are in fairly good agreement. The experimental pressure distribution for the NACA 64,3-440 airfoil section at $\alpha_o = 4^\circ$ (fig. 8) shows, however, a separated region at the trailing edge and, as a result, the experimental and theoretical pressure distributions differ appreciably. The application of leading-edge roughness increased the trailing-edge separation on both airfoil sections with a corresponding increase in the difference between the experimental and theoretical pressure distributions (figs. 7 and 8). The use of boundary-layer control eliminates trailing-edge separation at low angles of attack for both sections and, as a result, the experimental pressure distributions with boundary-layer control are in good agreement with the theoretical distributions except for the discontinuity at the slot.

The critial Mach number as determined from the theoretical pressure distribution for a lift coefficient of 0.4 is 0.527 and 0.462 for the NACA 64,2-432 and 64,3-440 airfoil sections, respectively, and, therefore, these sections would be most applicable to relatively low-speed airplanes.

Lift.- The NACA 64,2-432 and 64,3-440 airfoil sections have theoretical design lift coefficients of 0.4. The corresponding design angles of attack are 0° for the 32-percent-thick section and a value slightly different from 0° for the 40-percent-thick section. The difference in the design angle of attack for the two sections results from the modifications made to the $a = 1.0$ mean line employed in the 40-percent-thick section. Because of the trailing-edge separation which occurs even at low angles of attack on sections of such extreme thickness in the rough condition, the lift coefficient is negative at 0° angle of attack and the slope of the lift curve is quite irregular for both sections (figs. 9 and 10). The use of boundary-layer control, which delays turbulent trailing-edge separation, results in a more normal curve and, as the suction flow is increased, the near-linear part of the lift curve is extended to higher angles of attack with resultant increases in maximum lift coefficient. This effect of increasing suction on the maximum lift coefficient is more clearly shown in figure 14(a) where the maximum lift coefficient has been plotted as a function of

flow coefficient for the NACA 64,2-432 and 64,3-440 airfoil sections in the rough condition. Figure 14(a) shows that, for the NACA 64,2-432 airfoil section, a flow coefficient of approximately 0.003 is required before boundary-layer control becomes an effective means of increasing the maximum lift coefficient. From this point the maximum lift coefficient increased with increasing flow and reached a maximum of 2.57 at a flow coefficient of 0.038. The NACA 64,3-440 airfoil section required a flow coefficient of approximately 0.008 for boundary-layer control to become effective in increasing the maximum lift. From this point, the maximum lift coefficient increased with flow coefficient up to the maximum flow (C_Q = 0.032) available with the test equipment at which point a value of 3.49 was attained for the maximum lift coefficient. Thus, the maximum lift coefficient available with boundary-layer control increases with thickness ratio. This conclusion is in agreement with that of reference 3.

Drag.- The extensive region of trailing-edge separation, which was present on both models in the rough condition without suction, resulted in drags which were so large and erratic that they could not be measured with the equipment available. With boundary-layer control and the resultant delay in turbulent separation, however, the wake drag was sufficiently reduced to allow reliable measurement of the profile drag to be made. These measurements, which are presented in figures 9 to 13, indicate that the use of boundary-layer control is quite effective in reducing the wake drag and in maintaining low drag coefficients up to relatively high lift coefficients. As previously stated, the profile drag does not account for the boundary-layer-control suction power and, therefore, the total drags are also presented in figures 9 to 13. A comparison of the data presented in these figures with the data of reference 8 shows that, although the total-drag coefficients of the 32- and 40-percent-thick sections in the rough condition are large (the minimum values of the total drag coefficients are 0.017 and 0.028, respectively), they are not excessive for airfoil sections of such extreme thickness. The maximum ratios of section lift to total drag as determined from the data of figures 9 and 10 are presented in figure 15 as a function of flow coefficient. The maximum ratio of lift to total drag is approximately 59 for the NACA 64,2-432 airfoil and 42 for the NACA 64,3-440 airfoil section (see fig. 15). These maximum lift-drag ratios which occur at lift coefficients of 1.5 and 1.14, respectively, are comparable to section lift-drag ratios of much thinner sections with standard roughness (see reference 8) but occur at higher lift coefficients.

The data for the pressure loss through the suction slot used in calculating the drag equivalent of the boundary-layer-control suction power are presented in figures 9 to 12 in coefficient form and show that, for flow coefficients greater than about 0.02, the pressure loss increases rapidly with flow. Since the suction slots of these models were designed

for flow coefficients of 0.01 or less, it is likely that a more carefully designed slot and ducting system would result in less pressure loss. Any reduction in pressure loss thus accomplished would appear as a decrease in the total drag.

Effect of surface condition.- The effect of leading-edge roughness on the NACA 64,3-440 airfoil section was evaluated by comparing the section characteristics as presented in figures 10 and 11 for the rough and smooth condition, respectively. Figure 11 shows that the lift-curve slope for the smooth airfoil without suction is considerably less than the theoretical value of 0.15 and that the addition of leading-edge roughness (fig. 10) decreases the slope even more and increases the angle of zero lift. The data of figures 10 and 11 indicate that, in the leading-edge rough condition, suction becomes an effective means of increasing the slope of the lift curve of the section at much lower flow coefficients than in the smooth condition; however, for flow coefficients of 0.01 or more, the effect of roughness becomes slight and the slope of the lift curve approaches the theoretical value of 0.15 for both the smooth and rough condition. For the higher flow coefficients, the effect of leading-edge roughness on the maximum lift coefficient is negligible (see fig. 14(b)).

The addition of leading-edge roughness increases the wake drag at low suction flow coefficients ($C_Q < 0.02$) (figs. 10 and 11) but, for flow coefficients of 0.02 or more, the roughness effect on the wake drag is negligible. As a result of the increased slot pressure loss with leading-edge roughness, however, the total-drag coefficients are increased for all flow coefficients by the addition of leading-edge roughness (figs. 10(b) and 11(b)).

Slot position.- The effect of slot position on the lift and drag characteristics of the NACA 64,3-440 airfoil section with leading-edge roughness is shown by the data presented in figures 10 and 12 which are for the slot at 0.60c tested at a Reynolds number of 2.2×10^6 and for the slot at 0.50c tested at a Reynolds number of 3.0×10^6, respectively. The effect of the slight difference in Reynolds number of the two tests is believed to be negligible. From the data presented in figures 10, 12, and 14(c) it is seen that, for flow coefficients less than 0.02, suction at 0.50c was more effective in increasing the lift-curve slope and maximum lift coefficient than at 0.60c, and suction at 0.60c was more effective in reducing the minimum wake and total drag coefficients for the range of flow investigated; however, as a result of the larger maximum lift coefficients attained with the 0.50c-slot position, the maximum ratios of section lift to total drag, for the two slot positions, are approximately equal. The maximum ratio of section lift to total drag is 42 for the 0.60c-slot position and 41 for the 0.50c-slot position (see figs. 10 and 12).

Area suction.- Tests of the NACA 64,3-440 airfoil section with standard leading-edge roughness and with area suction extending from 0.55c to 0.71c were made at Reynolds numbers of 2.2×10^6 (fig. 13). The density of the porous material and the capacity of the boundary-layer-control blower limited this investigation to a maximum flow coefficient of 0.02. The data of figures 13 and 14(c) show that the lift-curve slope and maximum lift values increase more rapidly with small suction flow coefficients for the model with area suction than with a single slot; however, as the flow coefficient exceeds 0.01, suction at 0.50c becomes equally effective.

Figures 10, 12, and 13 show that, for low flow coefficients, the wake drag is less with area suction but, as a result of the large pressure loss through the porous material, the total drag with area suction is larger than for suction through a single slot at 0.50c or 0.60c. Further investigations with a material of greater porosity might result in lower total drag coefficients.

Effect of Boundary-Layer Control on Lift-Drag Ratio

As previously pointed out, the purpose in developing the airfoils of 32- and 40-percent chord in thickness was to determine whether, with the use of such airfoils together with boundary-layer control, some of the improvements in lift-drag ratio associated with high aspect ratios might be realized on structurally feasible wings. The data presented in the preceding discussion showed that boundary-layer control by suction was effective in reducing the total-drag coefficient of relatively thick airfoil sections and in increasing the section lift-drag ratio particularly in the high lift-coefficient range. Increases in the section lift-drag ratio in the high lift-coefficient range, however, are not necessarily indicative of corresponding increases in the lift-drag ratio of structurally feasible wings employing these sections. For this reason, the maximum lift-drag ratio has been calculated for a number of structurally feasible wings of varying aspect ratio and taper ratio. The wings investigated analytically varied in aspect ratio from 5 to 25 and in taper ratio from 0.2 to 1.0. All of the wings were considered to be untwisted, to have a tip-section thickness ratio of 0.12, and to vary linearly in absolute thickness from root to tip. A ratio of span to root thickness of 35 to 1 was chosen as being representative of existing cargo-type airplanes. If, however, the value of this ratio were increased, the maximum lift-drag ratio and optimum aspect ratio would also increase for the wings both with and without boundary-layer control. The root-section thickness ratio of a wing of aspect ratio 20 and taper ratio 0.2 is then about 0.34c. The calculations of the maximum lift-drag ratio were made by the method of reference 10. The section data used in the calculations for the wings with boundary-layer control, obtained from references 2, 3, 5, 6, 7, and from

the present paper, are presented in figure 16 in the form of total drag coefficient against thickness ratio for different lift coefficients. The section data for the wings without boundary-layer control are given in reference 8. All calculations were made from data for the rough-leading-edge condition. Since the roughness employed was probably more severe than that likely to be encountered under normal operating conditions, the calculated values of the maximum lift-drag ratio both with and without boundary-layer control may be somewhat low as compared with practical flight values. The drag equivalent of the boundary-layer control power was included in the calculations for the wings with boundary-layer control. After the wing drag was calculated as a function of lift coefficient for various combinations of aspect ratio and taper ratio, the maximum wing lift-drag ratio was found for the wing with and without boundary-layer control and is presented in figure 17 as a function of aspect ratio for the various taper ratios investigated. The wing lift coefficient at which the maximum lift-drag ratio occurs is presented in figure 18.

The results of the calculations, presented in figure 17, show that, for the wings investigated, the lift-drag ratio was not appreciably affected by the addition of boundary-layer control for aspect ratios of less than about 6. As the aspect ratio was increased beyond 6, however, the maximum lift-drag ratio of the wings with boundary-layer control increased more rapidly with aspect ratio than did that of the wings without boundary-layer control. This effect resulted in a maximum lift-drag ratio of 30.1 at a lift coefficient of 0.9 and an aspect ratio of 20 for the wing with a taper ratio of 0.2 and boundary-layer control; whereas, without boundary-layer control, the maximum lift-drag ratio was 26.6 at a lift coefficient of 0.5 and an aspect ratio of 12. Thus, the wing with boundary-layer control has a maximum lift-drag ratio which is approximately 13 percent greater than that of the wing without boundary-layer control. It should be emphasized that this gain does not depend on the possibility of obtaining any extensive laminar layers and includes the drag coefficient equivalent of the power required to operate the boundary-layer control. For the wings with and without boundary-layer control, the maximum lift-to-drag ratio increases with the taper ratio although the percentage increase in L/D due to boundary-layer control is not greatly affected by taper ratio for a given aspect ratio. Figure 19 shows the maximum lift-drag ratio as a function of aspect ratio for wings of various taper ratios both with and without boundary-layer control with an increment of parasite drag coefficient of 0.015 added to account for fuselage drag. Inspection of the data shows that a 20-percent increase in maximum lift-drag ratio results from the use of boundary-layer control in this case (that is, the use of boundary-layer control increases the maximum lift-drag ratio from 16.9 at a lift coefficient of 0.82 to 20.25 at a lift coefficient of 1.08 and increases the aspect ratio for maximum lift-drag ratio from 12.4 to 21).

The addition of a parasite drag coefficient of 0.015 also increases the optimum lift coefficient for maximum lift-drag ratio (figs. 18 and 20) and, from figures 17 and 19, the aspect ratio for maximum lift-drag ratio is found to increase slightly. The increases in $(L/D)_{max}$ due to boundary-layer control are greater in the case for which allowance is made for the parasite drag because the drag coefficient at $(L/D)_{max}$ is greater for the optimum wing with boundary-layer control than for the optimum wing without boundary-layer control. Consequently, the addition of a constant drag-coefficient increment to both wings results in a smaller percentage increase in the drag of the wing with boundary-layer control.

CONCLUSIONS

NACA 64-series airfoils with thickness ratios of 32- and 40-percent chord have been derived. Investigations have been made in the Langley two-dimensional low-turbulence tunnels to determine the effects of boundary-layer control by suction on the aerodynamic characteristics of the NACA 64,2-432 and 64,3-440 airfoil sections. In addition, an analysis was made to determine whether the maximum lift-drag ratio and the aspect ratio for maximum lift-drag ratio could be increased by the use of boundary-layer control on structurally feasible wings. The section data presented and employed in the analysis were obtained with standard roughness applied to the leading edges of the models. This roughness was probably more severe than that likely to be encountered on practical aircraft under normal operating conditions; therefore, the lift-drag ratios calculated from the section data may be somewhat low as compared with practical flight values. The results of these investigations indicate the following conclusions:

1. Large reductions in the wake-drag coefficient were obtained through a wide range of lift coefficient on the 32- and 40-percent-thick sections with relatively moderate flow coefficients and pressure-loss coefficients. The minimum total drag coefficients (including the drag coefficient equivalent of the suction power) for the 32- and 40-percent-thick sections in the rough surface condition were 0.017 and 0.028, respectively.

2. Wing characteristics as calculated from section data indicate that, for wings having a ratio of span to root thickness of 35 and a taper ratio of 0.2, the use of boundary-layer control increases the maximum lift-drag ratio by 13 percent, that is, from 26.6 at a lift coefficient of 0.5 to 30.1 at a lift coefficient of 0.9, and increases the aspect ratio for maximum lift-drag ratio from 12 to 20. With a parasite drag coefficient of 0.015 added to account for the drag of the

fuselage, tail, and so forth, the use of boundary-layer control increases the maximum lift-drag ratio by 20 percent, that is, from 16.9 at a lift coefficient of 0.82 to 20.25 at a lift coefficient of 1.08, and increases the aspect ratio for maximum lift-drag ratio from 12.4 to 21. These gains are based on calculations obtained by using section data corresponding to the rough surface condition and do not, therefore, depend on the attainment of extensive laminar layers.

3. Maximum lift coefficients of 2.57 and 3.49 were obtained for the 32- and 40-percent-thick sections without flaps for flow coefficients of 0.038 and 0.032, respectively.

4. The critical Mach numbers of the 32- and 40-percent-thick sections as determined from the theoretical pressure distributions at a lift coefficient of 0.4 were 0.527 and 0.462, respectively. These sections would, therefore, have application to relatively low-speed, long-range aircraft.

Langley Aeronautical Laboratory
National Advisory Committee for Aeronautics
Langley Field, Va., November 30, 1950

REFERENCES

1. Neely, Robert H., Bollech, Thomas V., Westrick, Gertrude C., and Graham, Robert R.: Experimental and Calculated Characteristics of Several NACA 44-Series Wings with Aspect Ratios of 8, 10, and 12 and Taper Ratios of 2.5 and 3.5. NACA TN 1270, 1947.

2. Quinn, John H., Jr.: Tests of the NACA 64_1A212 Airfoil Section with a Slat, a Double Slotted Flap, and Boundary-Layer Control by Suction. NACA TN 1293, 1947.

3. Horton, Elmer A., Racisz, Stanley F., and Paradiso, Nicholas J.: Investigation of Boundary-Layer Control to Improve the Lift and Drag Characteristics of the NACA 65_2-415 Airfoil Section with Double Slotted and Plain Flaps. NACA TN 2149, 1950.

4. Quinn, John H., Jr.: Tests of the NACA 65_3-018 Airfoil Section with Boundary-Layer Control by Suction. NACA CB L4H10, 1944.

5. Quinn, John H., Jr.: Wind-Tunnel Investigation of Boundary-Layer Control by Suction on the NACA 65_3-418, a = 1.0 Airfoil Section with a 0.29-Airfoil-Chord Double Slotted Flap. NACA TN 1071, 1946.

6. Quinn, John H., Jr.: Wind-Tunnel Investigation of the NACA 65_4-421 Airfoil Section with a Double Slotted Flap and Boundary-Layer Control by Suction. NACA TN 1395, 1947.

7. Racisz, Stanley F., and Quinn, John H., Jr.: Wind-Tunnel Investigation of Boundary-Layer Control by Suction on NACA 65_5-424 Airfoil with Double Slotted Flap. NACA TN 1631, 1948.

8. Abbott, Ira H., Von Doenhoff, Albert E., and Stivers, Louis S., Jr.: Summary of Airfoil Data. NACA Rep. 824, 1945. (Formerly NACA ACR L5C05.)

9. Von Doenhoff, Albert E., and Abbott, Frank T., Jr.: The Langley Two-Dimensional Low-Turbulence Pressure Tunnel. NACA TN 1283, 1947.

10. Anderson, Raymond F.: Determination of the Characteristics of Tapered Wings. NACA Rep. 572, 1936.

TABLE I

ORDINATES FOR THE NACA 64,2-432 AIRFOIL SECTION

[Stations and ordinates in percent airfoil chord]

Upper surface		Lower surface	
Station	Ordinate	Station	Ordinate
0	0	0	0
-.022	3.198	1.022	-2.998
.162	3.924	1.338	-3.644
.579	5.036	1.921	-4.608
1.730	6.978	3.270	-6.234
4.164	9.554	5.836	-8.290
6.661	11.344	8.339	-9.648
9.182	12.729	10.818	-10.661
14.260	14.753	15.740	-12.061
19.357	16.168	20.643	-12.984
24.463	17.148	25.537	-13.568
29.573	17.763	30.427	-13.875
34.685	18.057	35.315	-13.937
39.795	18.019	40.205	-13.735
44.902	17.551	45.098	-13.171
50.000	16.716	50.000	-12.304
55.085	15.568	54.915	-11.188
60.155	14.140	59.845	-9.856
65.205	12.485	64.795	-8.365
70.235	10.661	69.765	-6.773
75.239	8.633	74.761	-5.053
80.228	6.760	79.772	-3.576
85.192	4.819	84.808	-2.127
90.136	2.976	89.864	-.908
95.066	1.334	94.934	-.070
100.000	0	100.000	0

L.E. radius: 10.146
Slope of radius through L.E.: 0.1685

TABLE II

ORDINATES FOR THE NACA 64,3-440 a=1.0 (modified)

AIRFOIL SECTION

[Stations and ordinates in percent airfoil chord]

Upper surface		Lower surface	
Station	Ordinate	Station	Ordinate
0	0	0	0
-.078	4.333	1.078	-4.195
.076	5.149	1.424	-4.943
.443	6.409	2.057	-6.073
1.504	8.675	3.496	-8.027
3.874	11.717	6.126	-10.519
6.377	13.920	8.623	-12.256
8.934	15.642	11.066	-13.582
14.072	18.155	15.928	-15.463
19.195	19.851	20.805	-16.667
24.329	20.983	25.671	-17.403
29.466	21.730	30.534	-17.842
34.606	22.056	35.394	-17.936
39.745	21.917	40.255	-17.633
44.878	21.310	45.122	-16.930
50.000	20.238	50.000	-15.826
55.106	18.743	54.894	-14.363
60.190	16.893	59.810	-12.609
65.250	14.765	64.750	-10.645
70.284	12.463	69.716	-8.575
75.290	10.094	74.710	-6.514
80.270	7.722	79.730	-4.538
85.225	5.425	84.775	-2.733
90.158	3.294	89.842	-1.226
95.076	1.444	94.924	-.180
100.000	0	100.000	0

L.E. radius: 14.050
Slope of radius through L.E.: 0.168

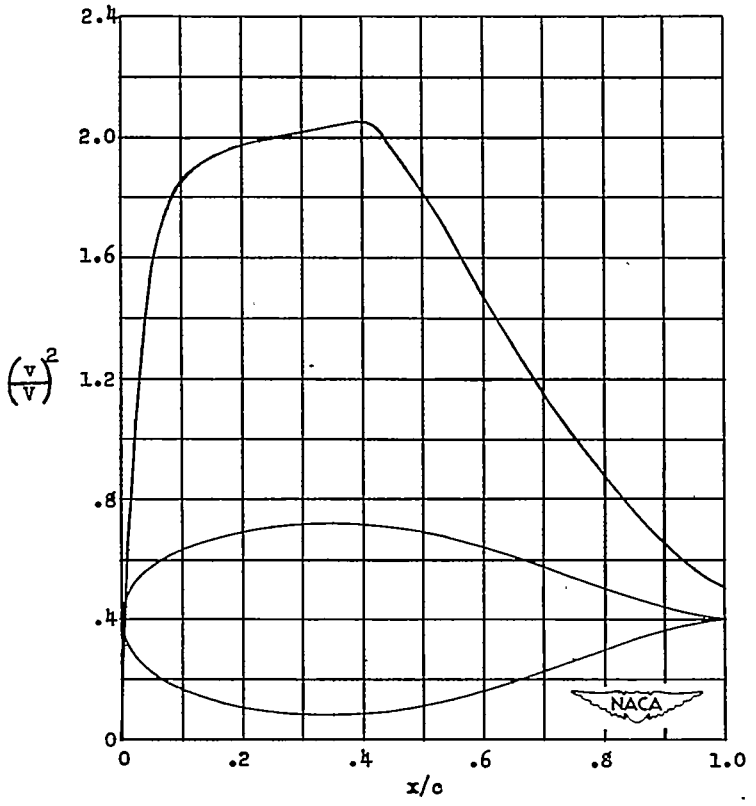

x (percent c)	y (percent c)	$(v/V)^2$	v/V	$\Delta v_a/V$
0	0	0	0	.821
.5	3.142	.310	.557	.800
.75	3.829	.442	.665	.789
1.25	4.868	.630	.794	.766
2.5	6.651	1.029	1.014	.711
5	8.961	1.545	1.243	.602
7.5	10.529	1.747	1.322	.516
10	11.724	1.858	1.363	.453
15	13.427	1.928	1.389	.371
20	14.590	1.968	1.403	.314
25	15.367	1.997	1.413	.274
30	15.825	2.019	1.421	.243
35	16.000	2.039	1.428	.216
40	15.878	2.053	1.433	.192
45	15.361	1.959	1.400	.168
50	14.510	1.809	1.345	.145
55	13.378	1.646	1.283	.124
60	11.999	1.478	1.216	.104
65	10.427	1.310	1.145	.087
70	8.720	1.153	1.074	.072
75	6.847	1.010	1.005	.059
80	5.173	.881	.939	.048
85	3.478	.764	.874	.036
90	1.947	.662	.814	.026
95	.705	.572	.756	.017
100	0	.502	.709	0
L. E. radius: 10.146 percent c				

Figure 1.- Theoretical pressure distribution and ordinates of the basic thickness form of the NACA 64,2-032 airfoil section.

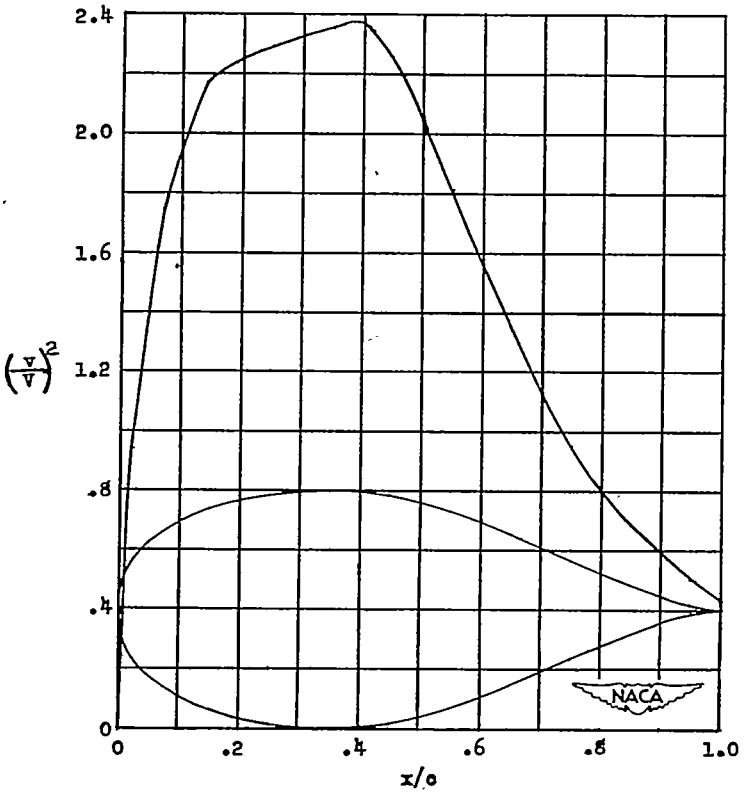

x (percent c)	y (percent c)	$(v/V)^2$	v/V	$\Delta v_a/V$
0	0	0	0	0.666
.5	4.303	.275	.524	.664
.75	5.091	.400	.632	.662
1.25	6.293	.560	.748	.653
2.5	8.410	.940	.970	.619
5	11.175	1.445	1.202	.543
7.5	13.136	1.760	1.327	.486
10	14.651	1.937	1.392	.441
15	16.835	2.198	1.483	.367
20	18.277	2.256	1.502	.314
25	19.205	2.293	1.514	.273
30	19.793	2.325	1.525	.242
35	20.000	2.351	1.533	.216
40	19.777	2.372	1.540	.190
45	19.120	2.255	1.502	.165
50	18.032	2.040	1.428	.142
55	16.553	1.809	1.345	.119
60	14.752	1.563	1.250	.098
65	12.707	1.340	1.158	.080
70	10.523	1.128	1.062	.064
75	8.309	.950	.975	.052
80	6.136	.813	.902	.041
85	4.085	.696	.834	.031
90	2.266	.592	.769	.022
95	.816	.504	.710	.014
100	0	.431	.657	0
L. E. radius: 14.050 percent c				

Figure 2.- Theoretical pressure distribution and ordinates of the basic thickness form of the NACA 64,3-040 airfoil section.

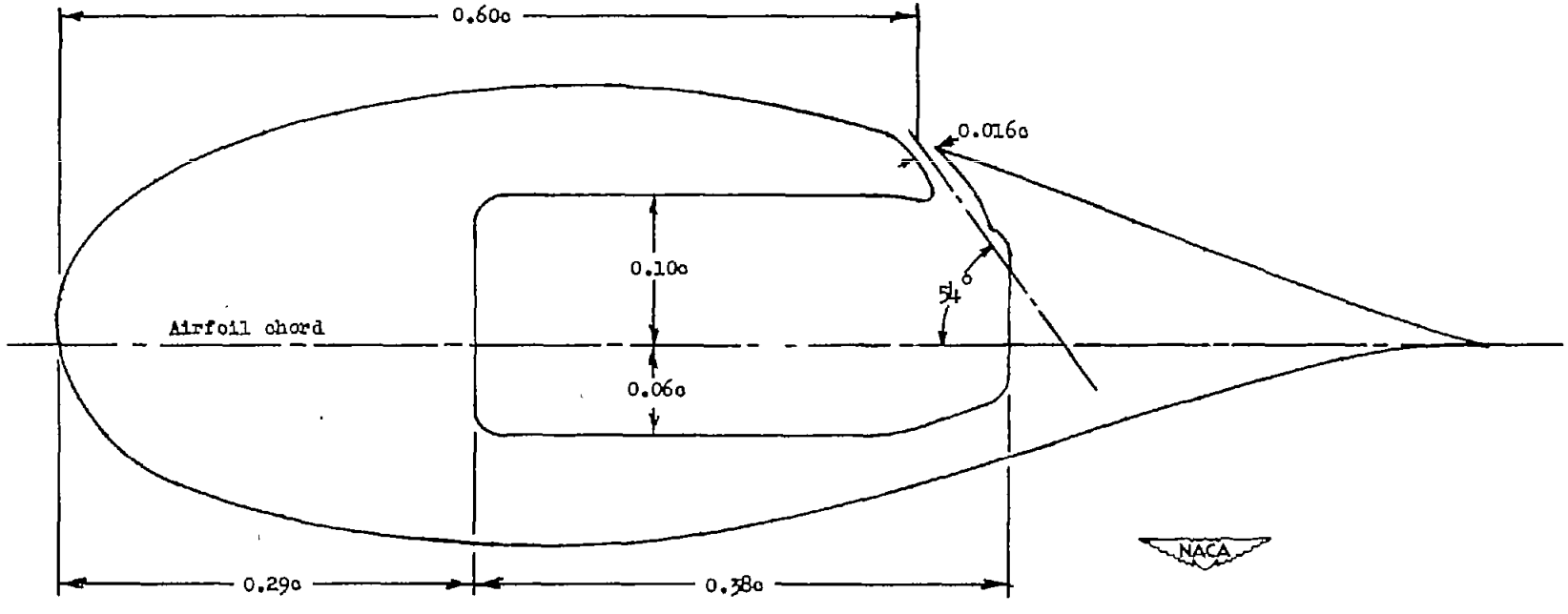

Figure 3.- Profile of the NACA 64,2-432 airfoil section with a boundary-layer-control slot at 0.60c.

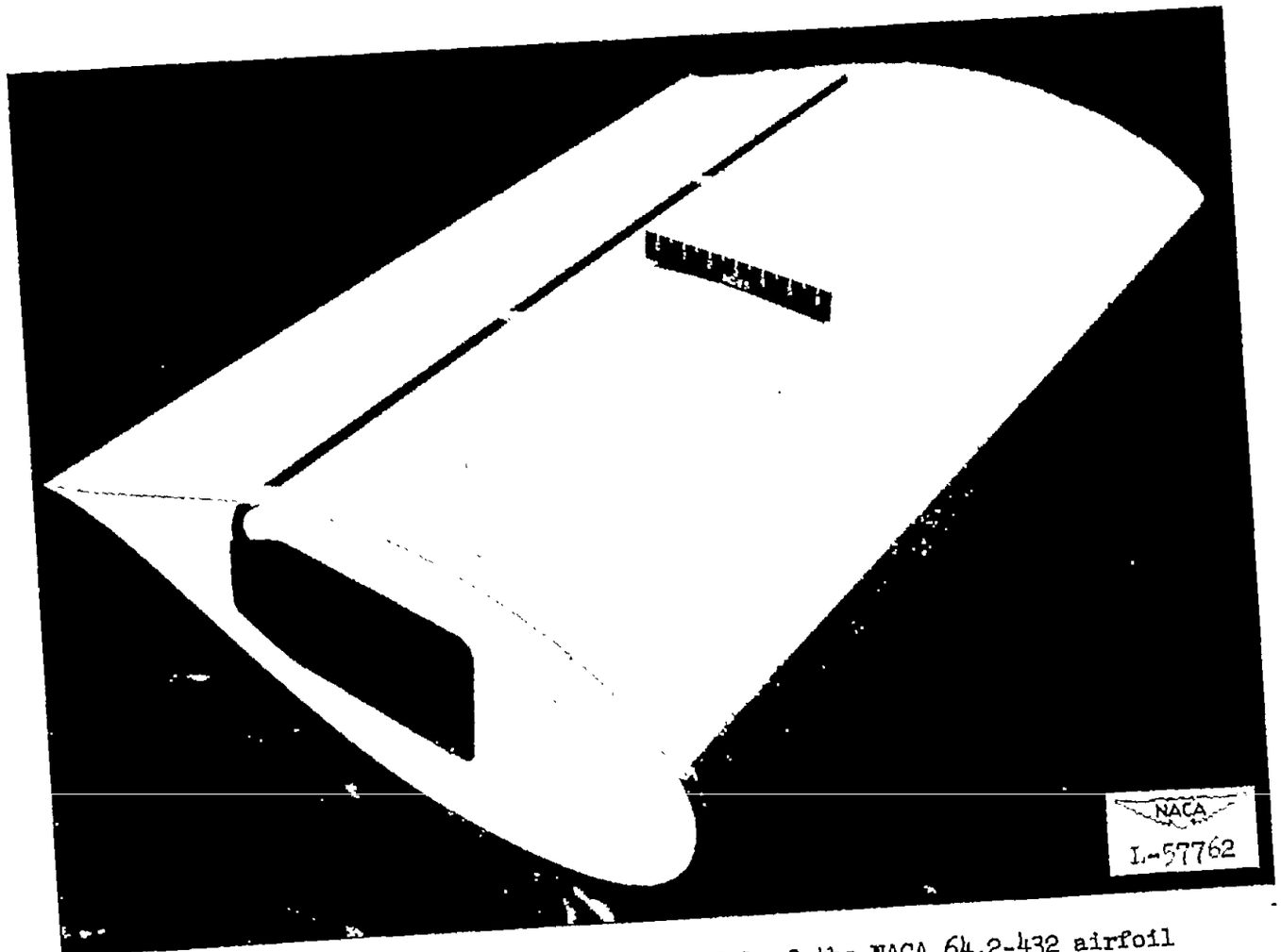

Figure 4.- Three-quarter view of the model of the NACA 64,2-432 airfoil section with a 0.016c boundary-layer-control slot at 0.60c and leading-edge roughness.

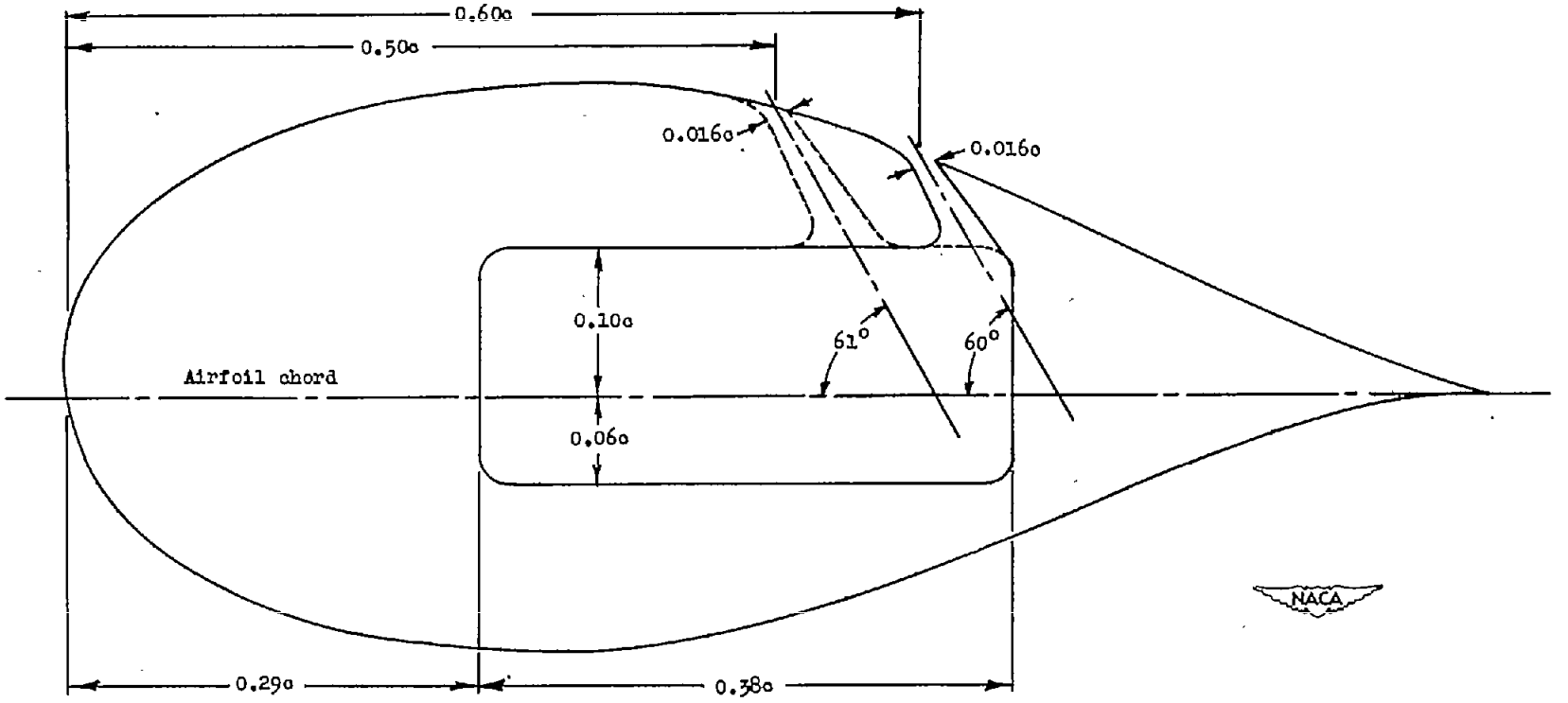

Figure 5.- Profile of the NACA 64,3-440 airfoil section with the two boundary-layer-control slots tested.

Figure 6.- Three-quarter view of the model of the NACA 64,3-440 airfoil section with a porous upper surface from 0.55c to 0.71c and leading-edge roughness.

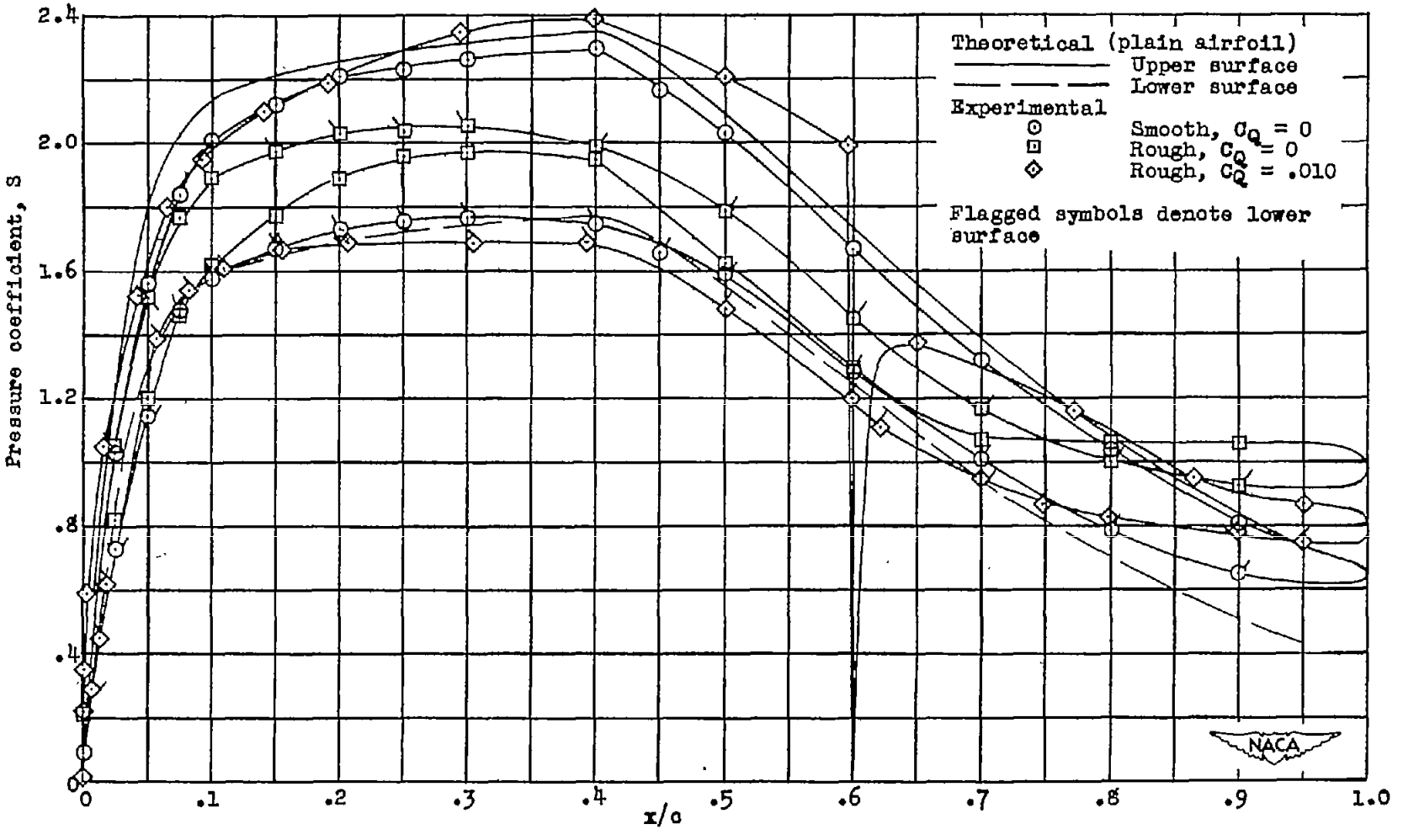

Figure 7.- A comparison of the theoretical and experimental pressure distributions on the NACA 64,2-432 airfoil section at $\alpha_o = 0^\circ$ and data to show the effect of roughness and boundary-layer control. $R = 2.2 \times 10^6$.

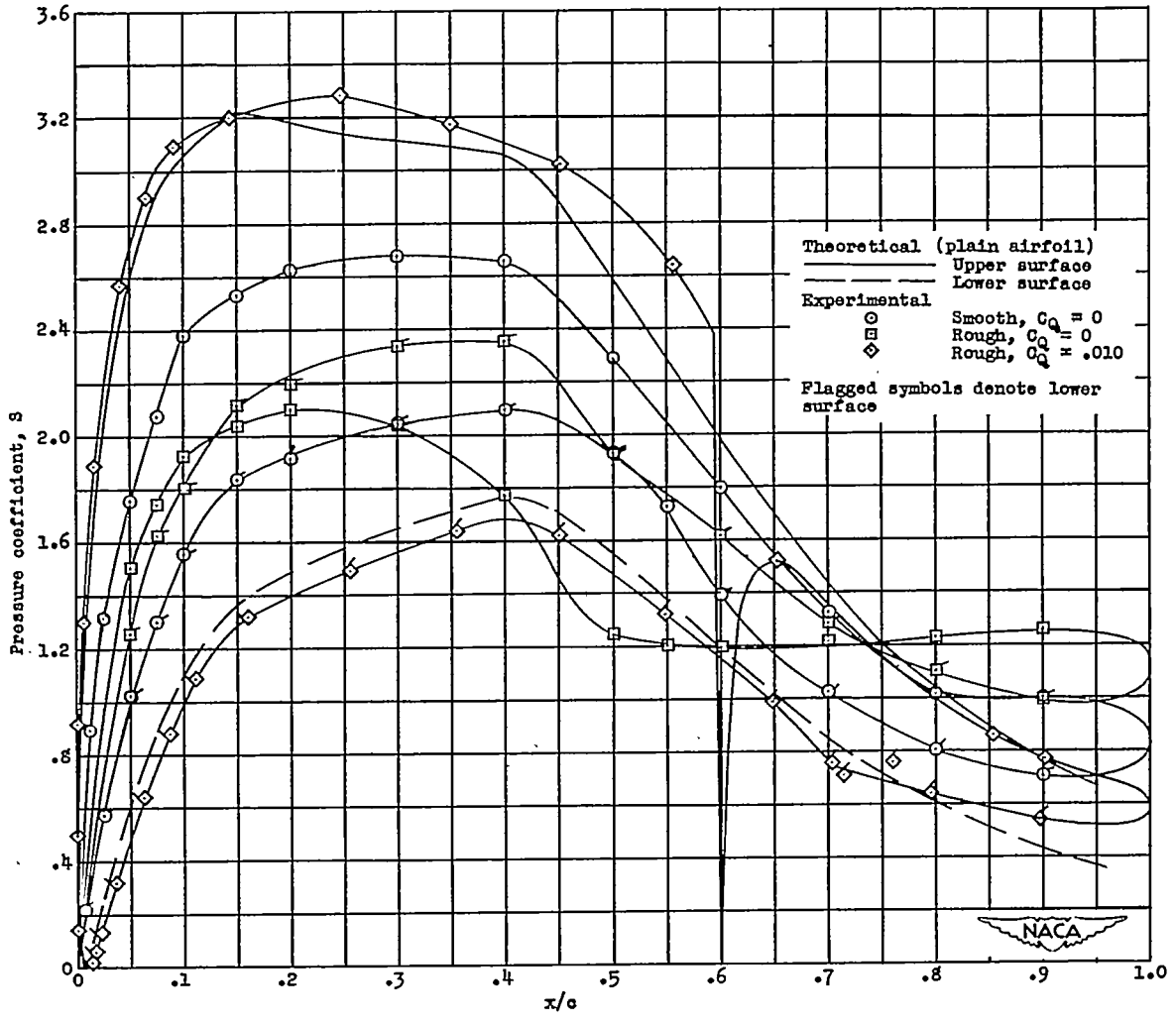

Figure 8.- A comparison of the theoretical and experimental pressure distributions on the NACA 64,3-440 airfoil section at $\alpha_o = 4^o$ and data to show the effect of roughness and boundary-layer control. $R = 2.2 \times 10^6$.

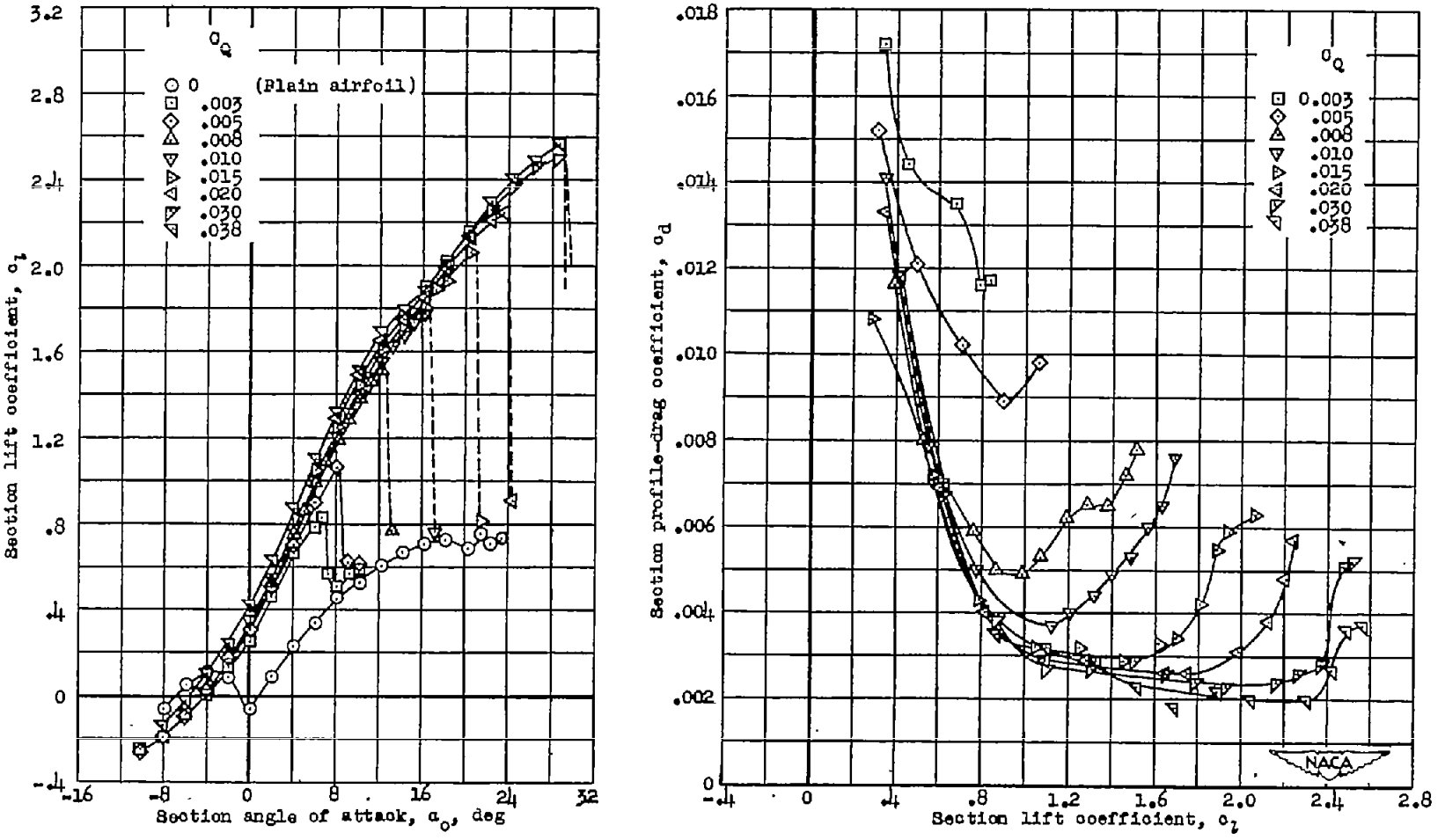

(a) Lift and profile drag.

Figure 9.- Airfoil section characteristics of the NACA 64,2-432 airfoil section with a 0.016c boundary-layer-control slot at 0.60c. Model in rough condition; $R = 2.2 \times 10^6$.

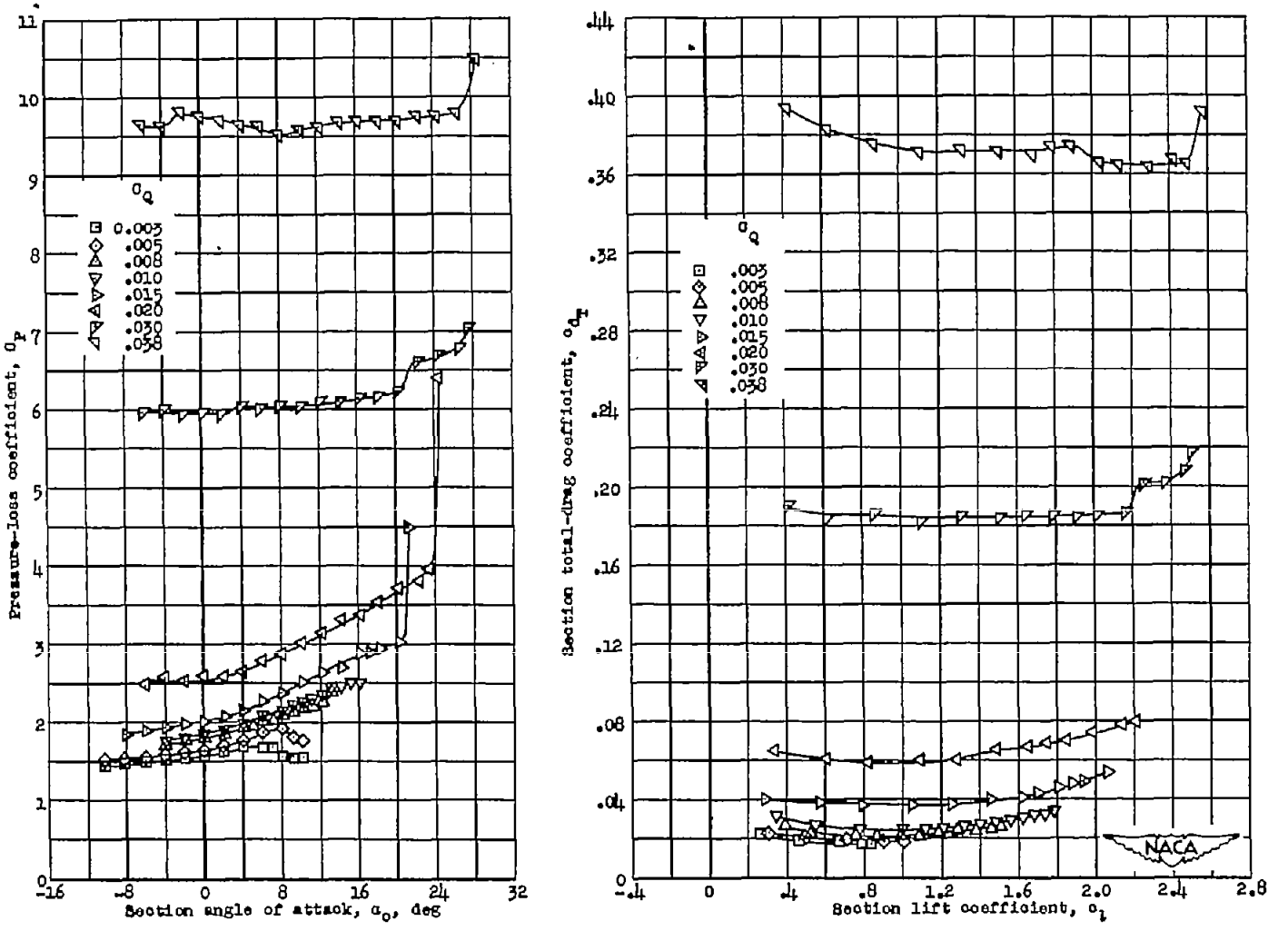

(b) Pressure loss and total drag.

Figure 9.- Concluded.

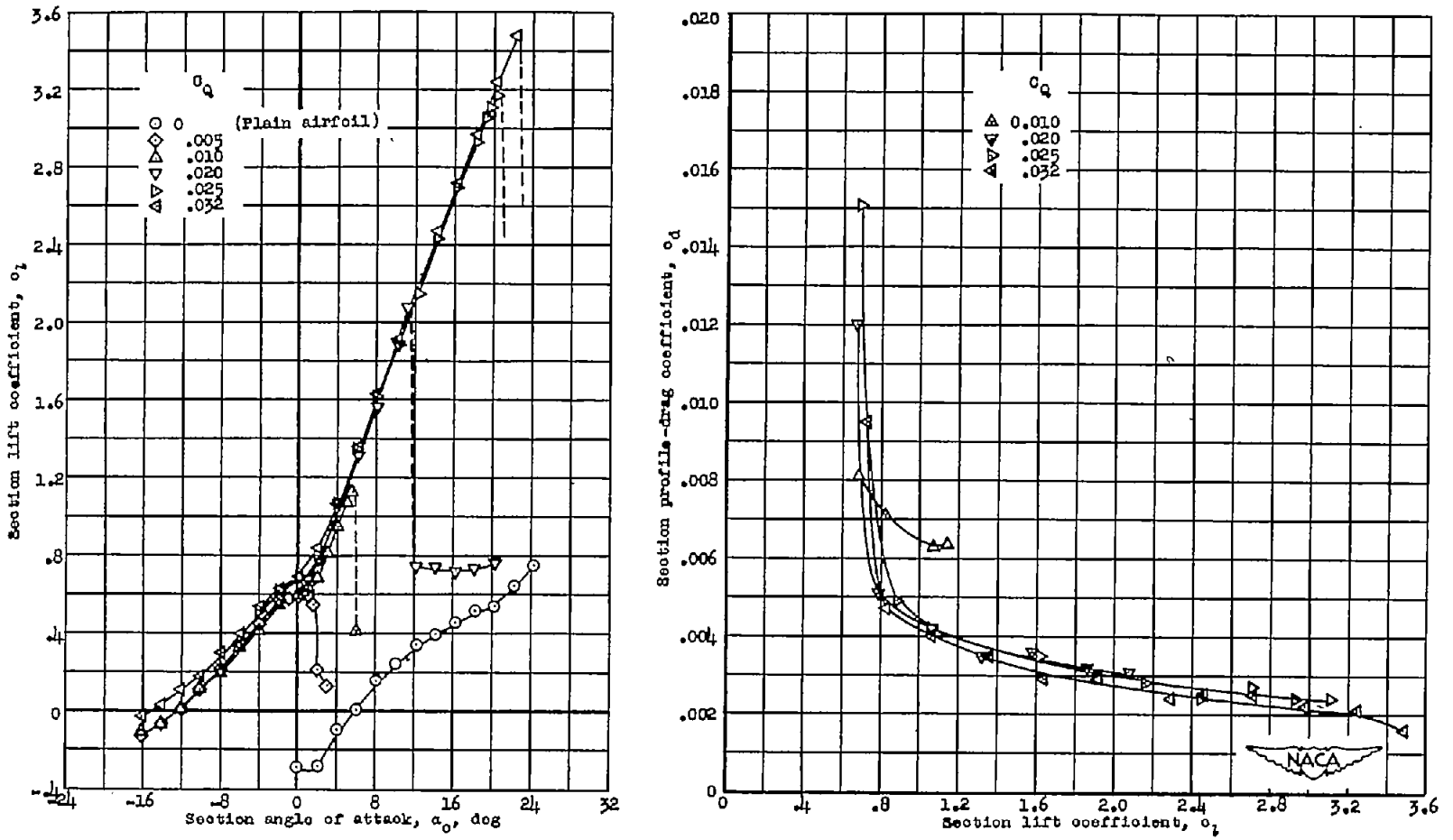

(a) Lift and profile drag.

Figure 10.- Airfoil section characteristics of the NACA 64,3-440 airfoil section with a 0.016c boundary-layer-control slot at 0.60c. Model in rough condition; $R = 2.2 \times 10^6$.

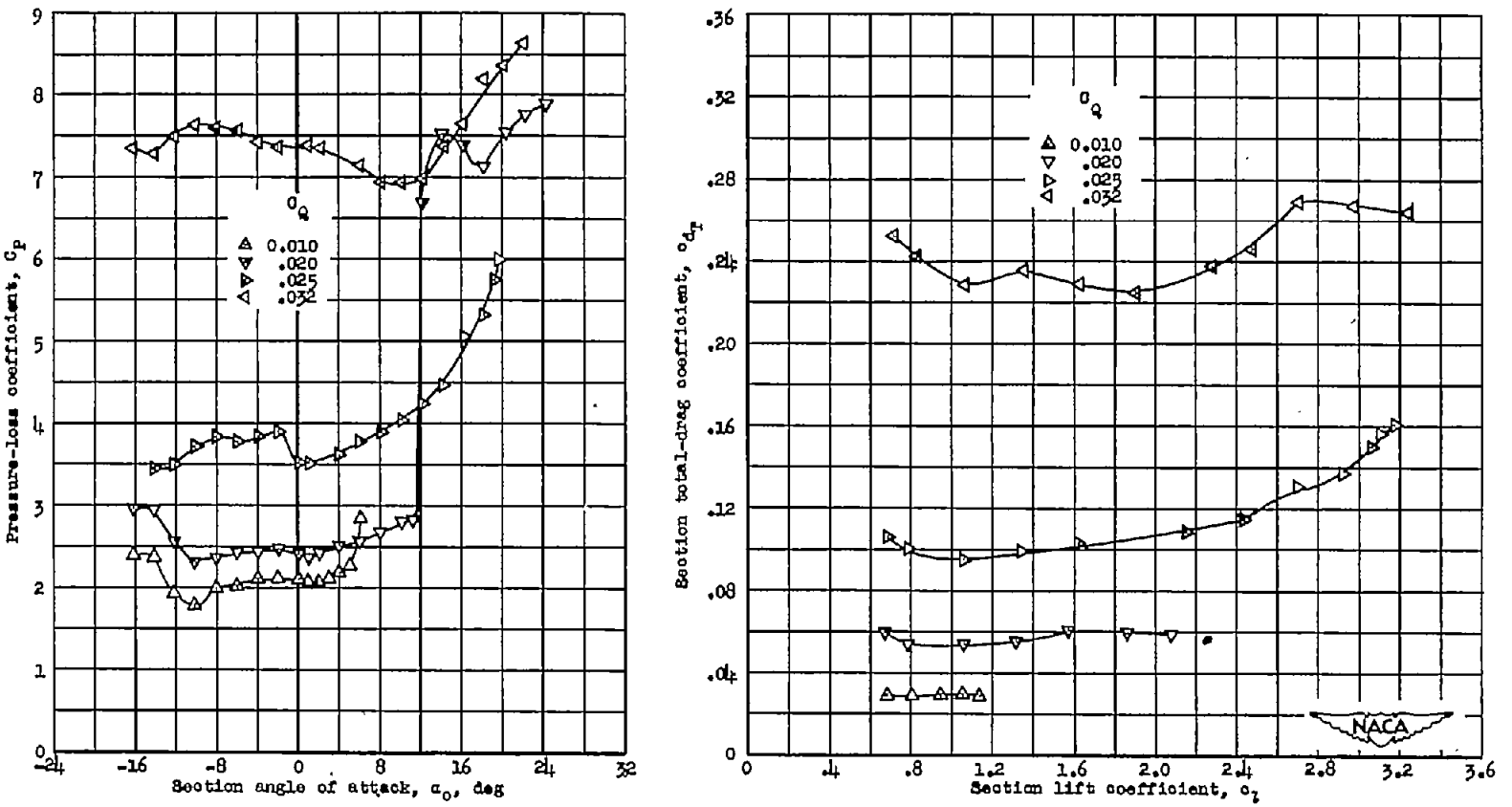

(b) Pressure loss and total drag.

Figure 10.- Concluded.

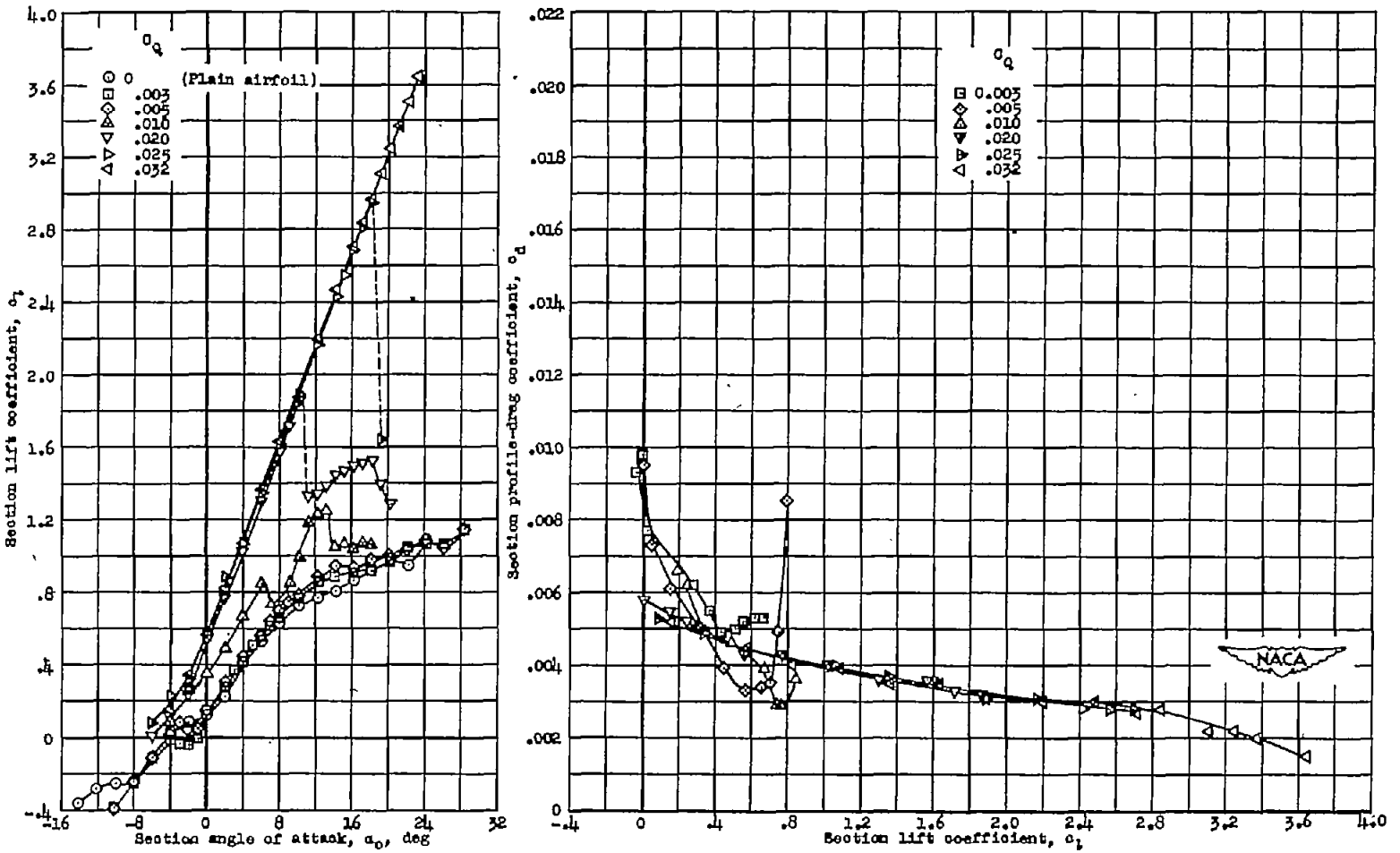

(a) Lift and profile drag.

Figure 11.- Airfoil section characteristics of the NACA 64,3-440 airfoil section with a 0.016c boundary-layer-control slot at 0.60c. Model in smooth condition; $R = 2.2 \times 10^6$.

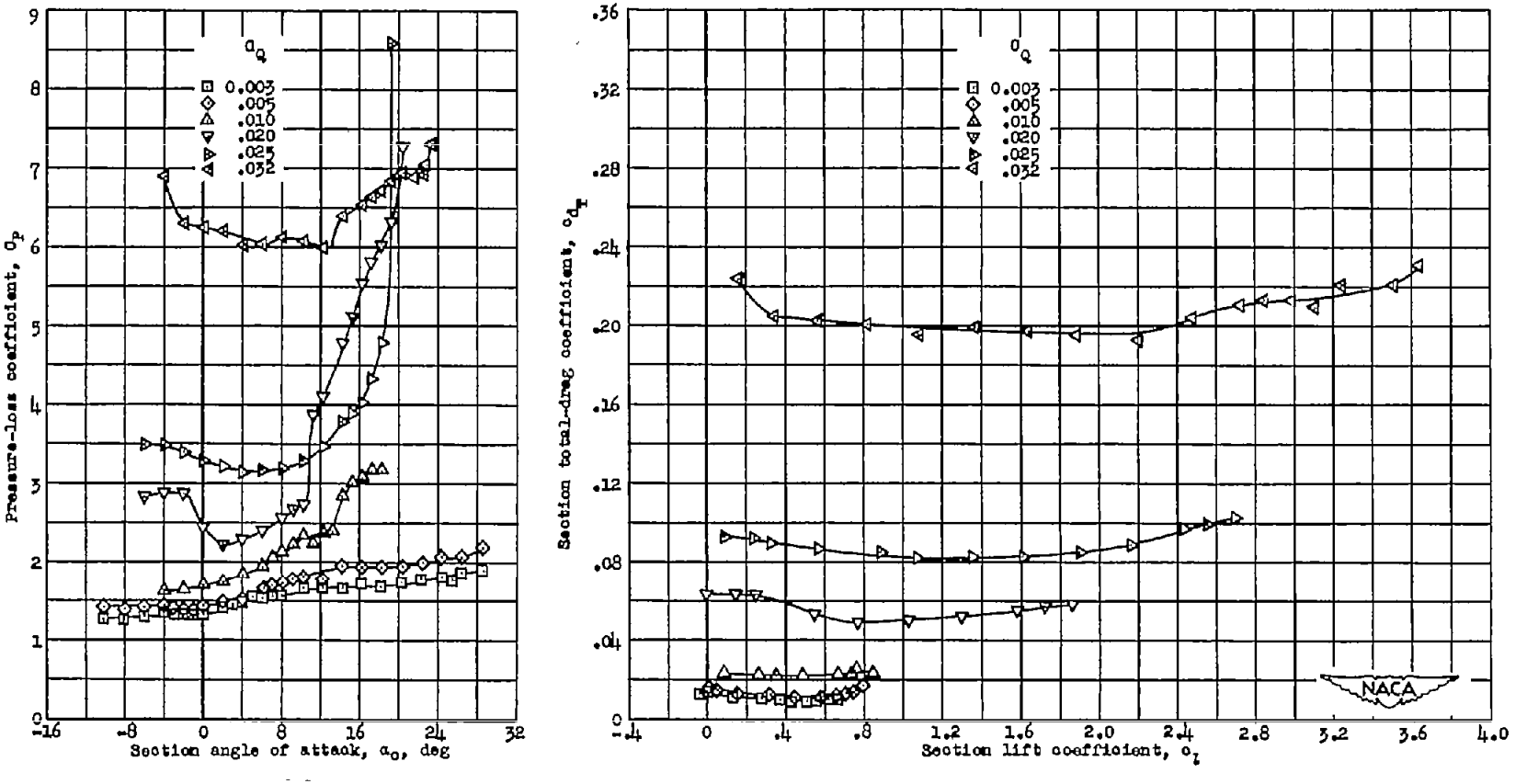

(b) Pressure loss and total drag.

Figure 11.- Concluded.

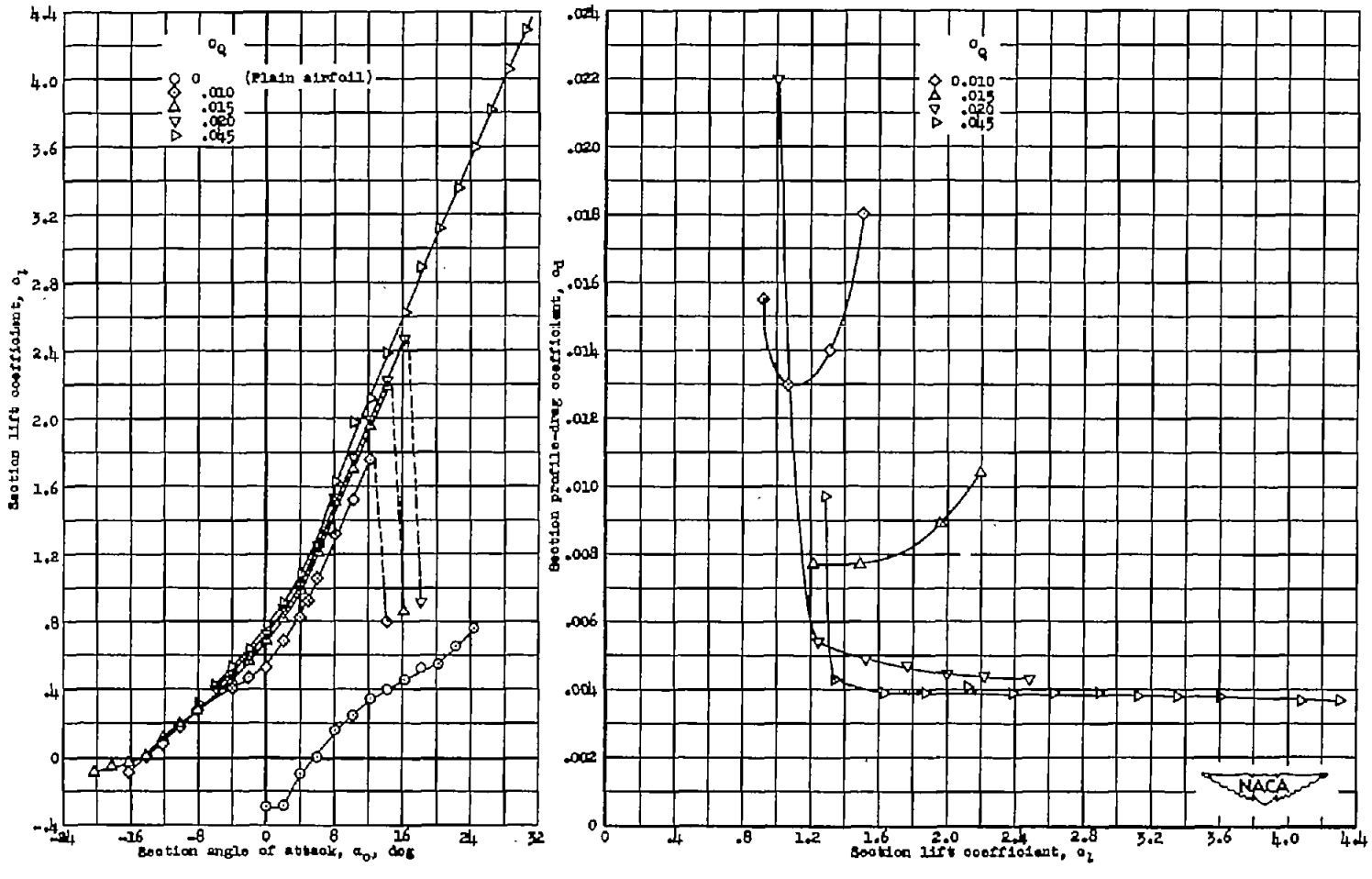

(a) Lift and profile drag.

Figure 12.- Airfoil section characteristics of the NACA 64,3-440 airfoil section with a 0.016c boundary-layer-control slot at 0.50c. Model in rough condition; $R = 3.0 \times 10^6$.

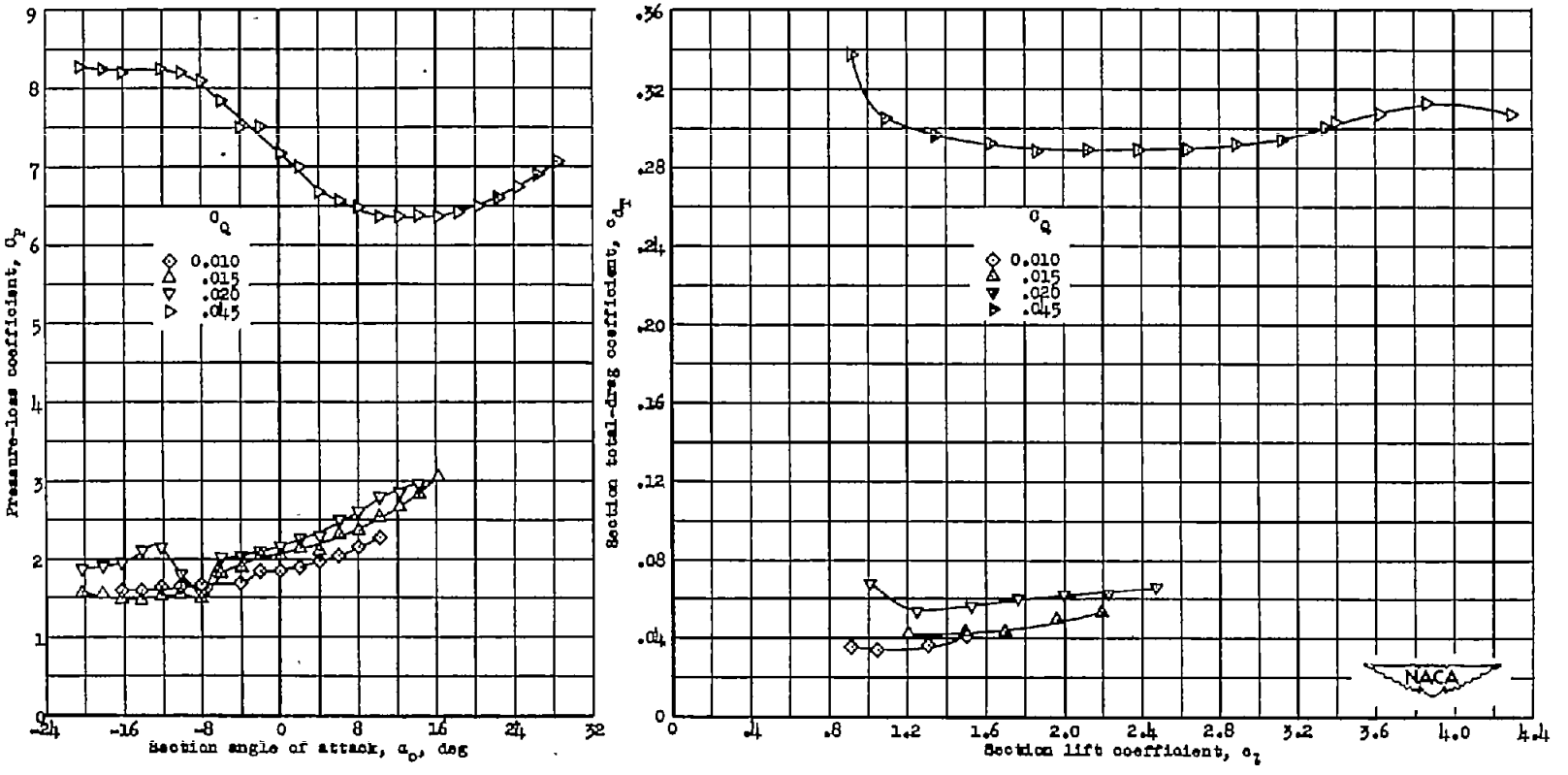

(b) Pressure loss and total drag.

Figure 12.- Concluded.

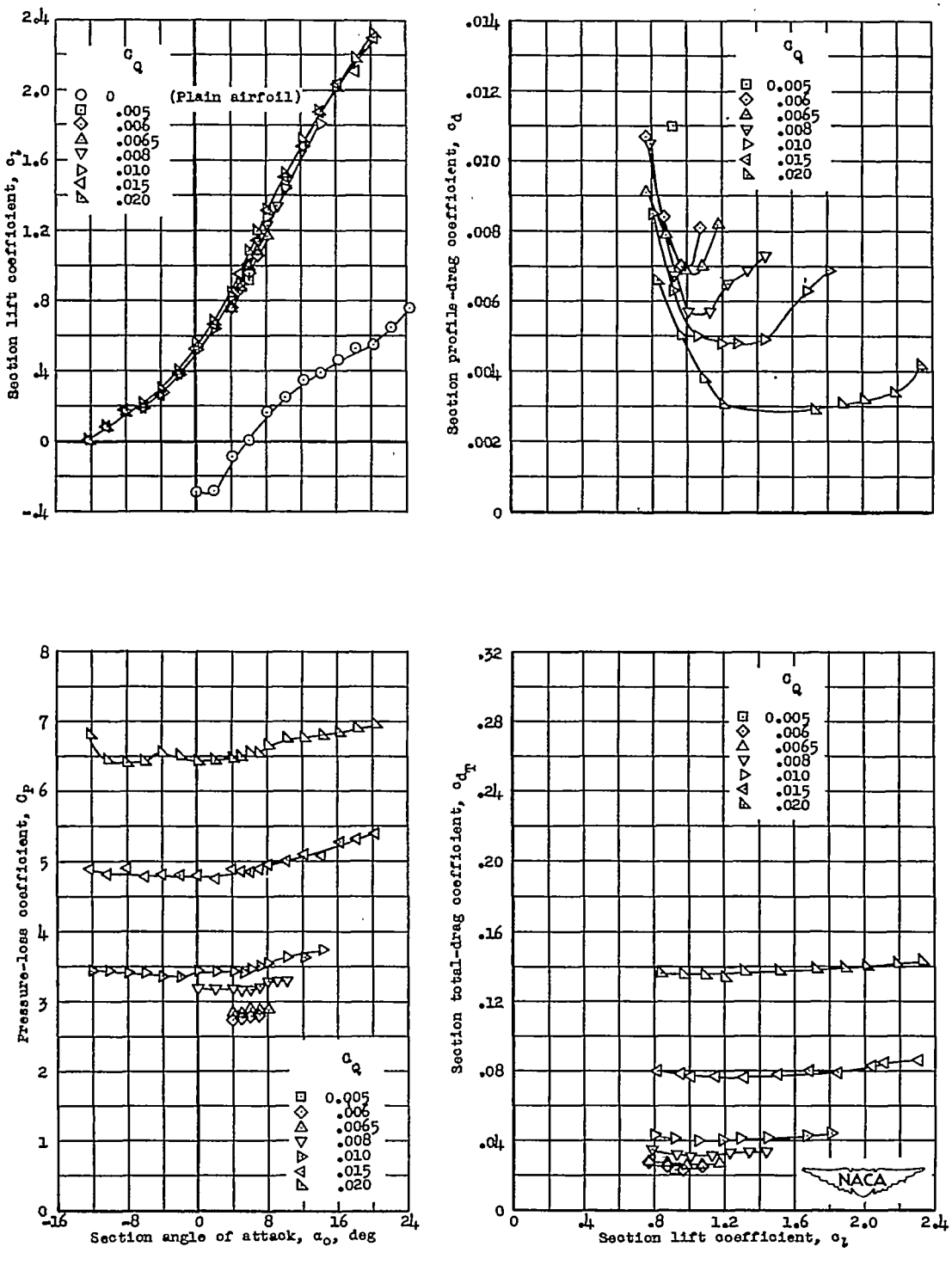

Figure 13.- Airfoil section characteristics of the NACA 64,3-440 airfoil section with boundary-layer control by means of a porous upper surface from 0.55c to 0.71c. Model in rough condition; $R = 2.2 \times 10^6$.

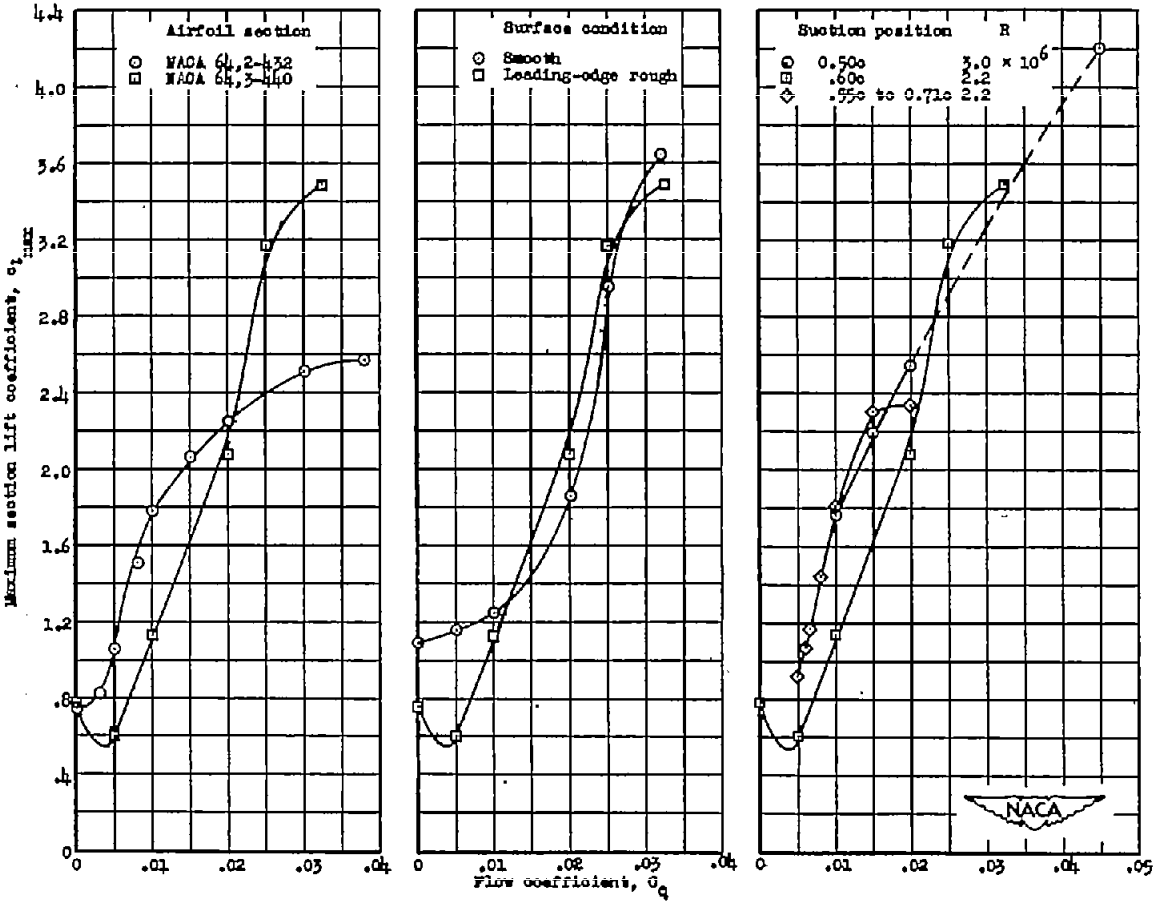

(a) Effect of airfoil thickness; slot at 0.60c; models in rough condition; $R = 2.2 \times 10^6$.

(b) Effect of surface condition; NACA 64,3-440 airfoil; slot at 0.60c; $R = 2.2 \times 10^6$.

(c) Effect of position of suction; NACA 64,3-440 airfoil; rough condition.

Figure 14.- Effects of several variables on variation of maximum section lift coefficient with flow coefficient.

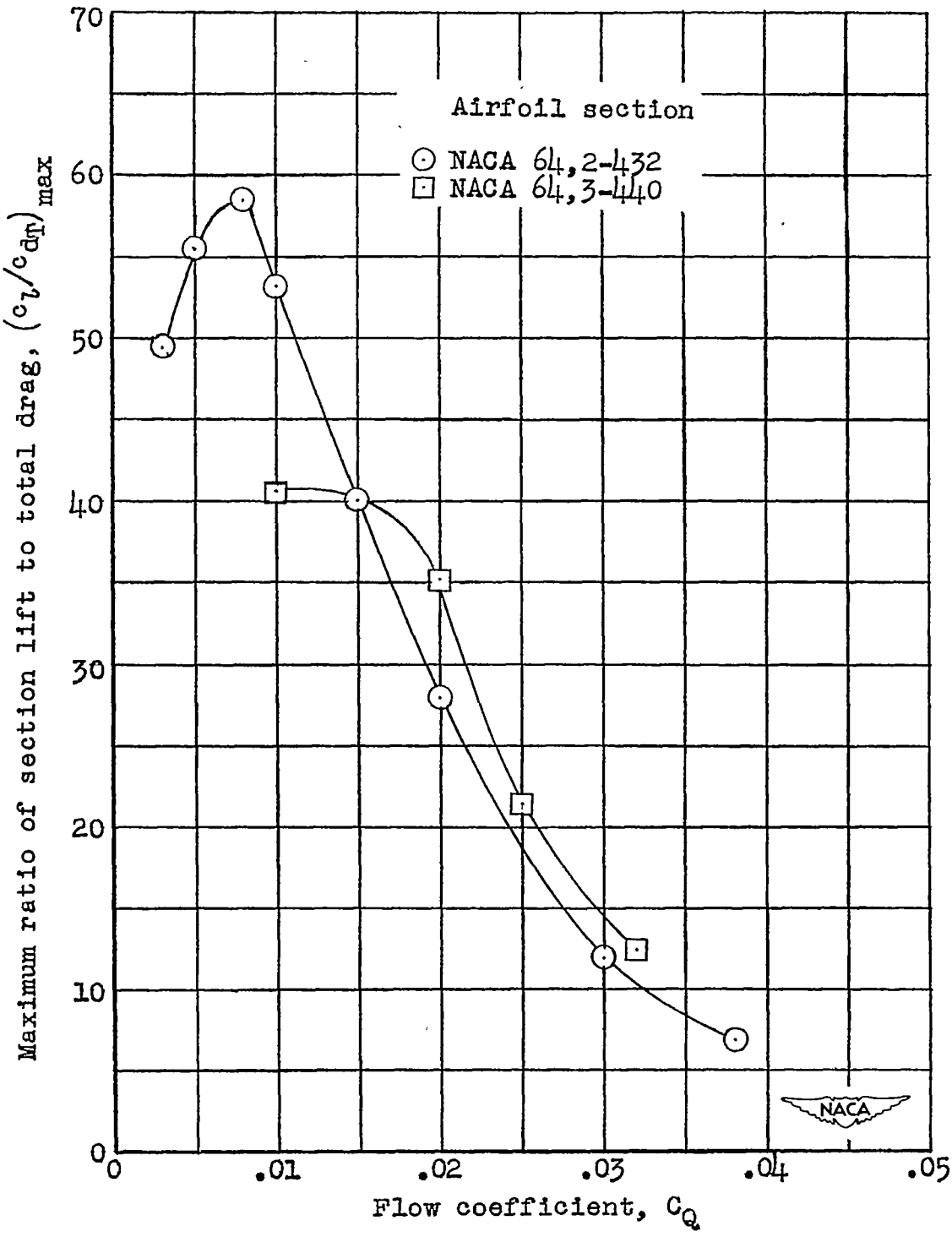

Figure 15.- Effect of flow coefficient on the maximum ratio of section lift to total drag of the NACA 64,2-432 and 64,3-440 airfoil sections. Suction slot at 0.60c; $R = 2.2 \times 10^6$.

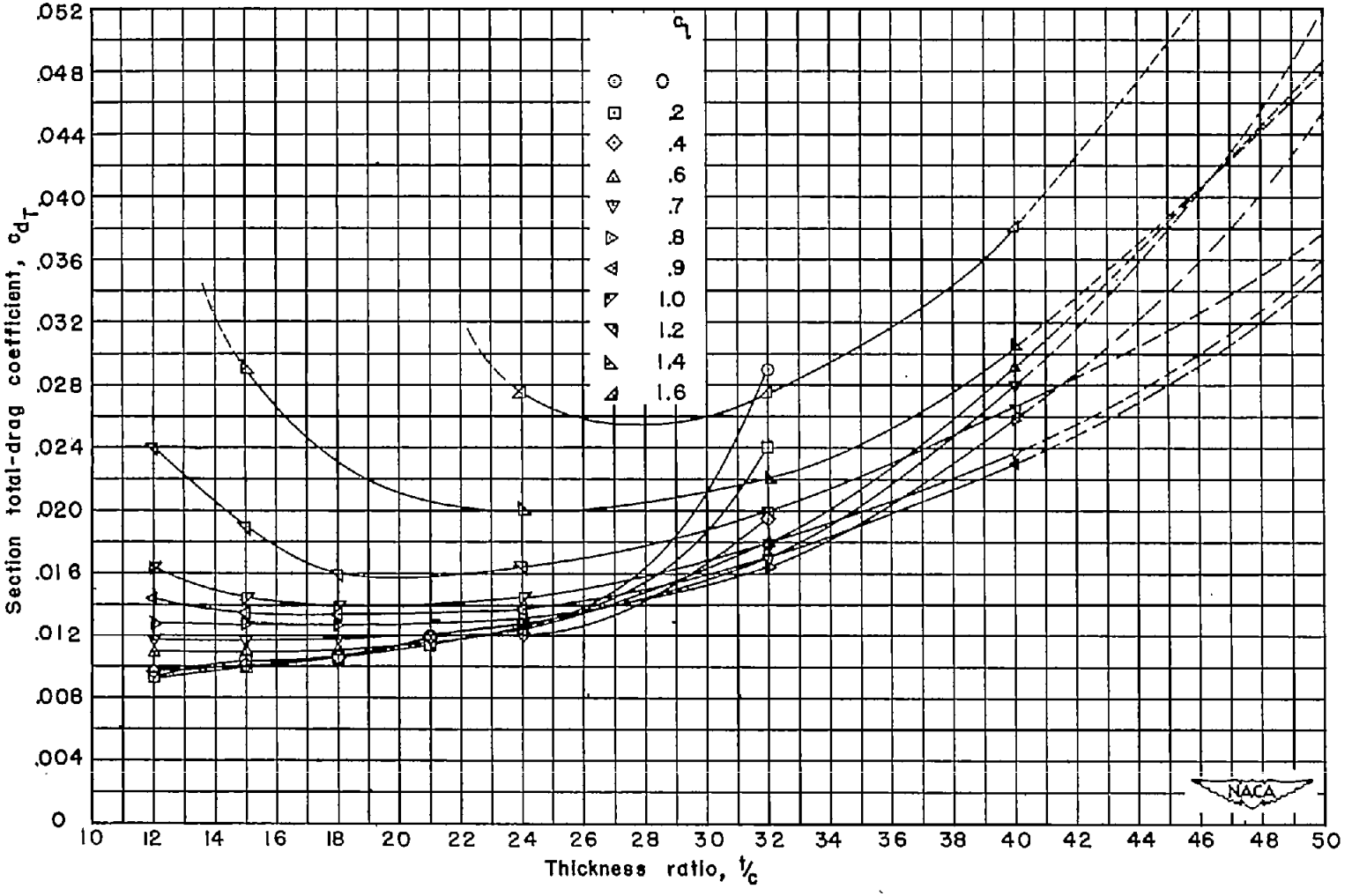

Figure 16. Effect of thickness ratio on the section total-drag characteristics of NACA 64-series airfoil sections with boundary-layer control for various lift coefficients.

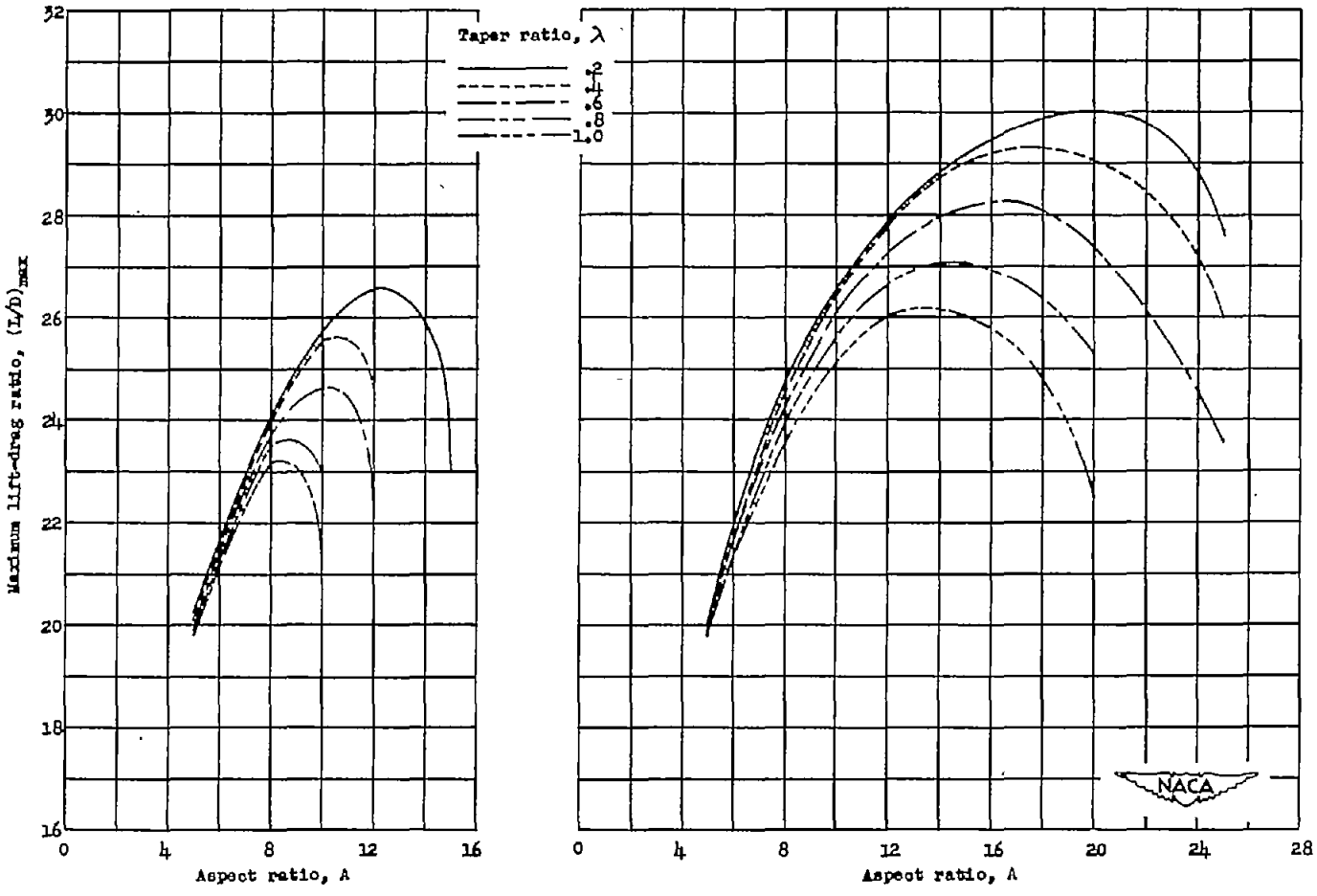

(a) Wing without boundary-layer control.

(b) Wing with boundary-layer control.

Figure 17.- Effect of aspect ratio on the maximum lift-drag ratio of a family of wings of various taper ratios with and without boundary-layer control.

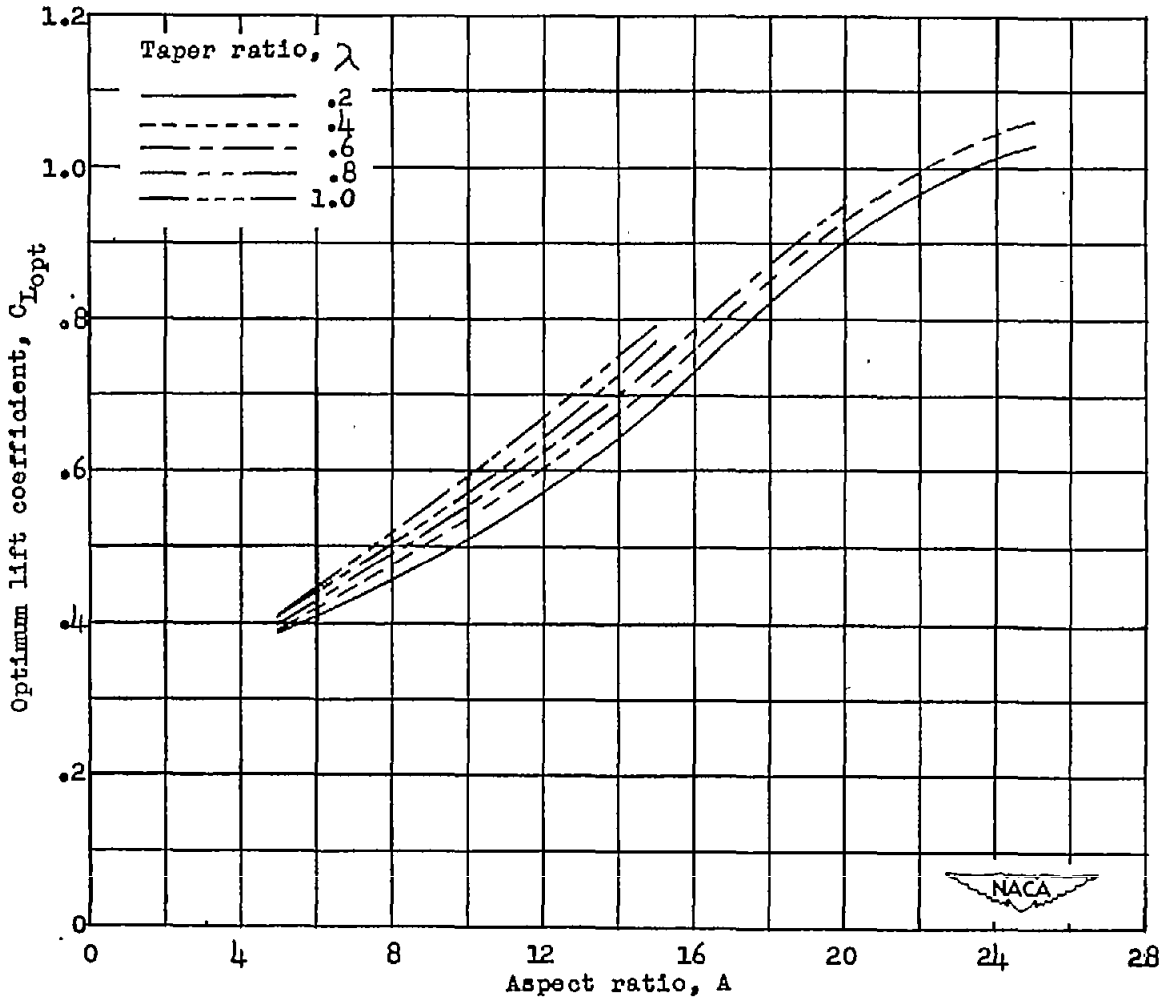

Figure 18.- Variation of optimum lift coefficient with aspect ratio for a family of wings of various taper ratios with boundary-layer control.

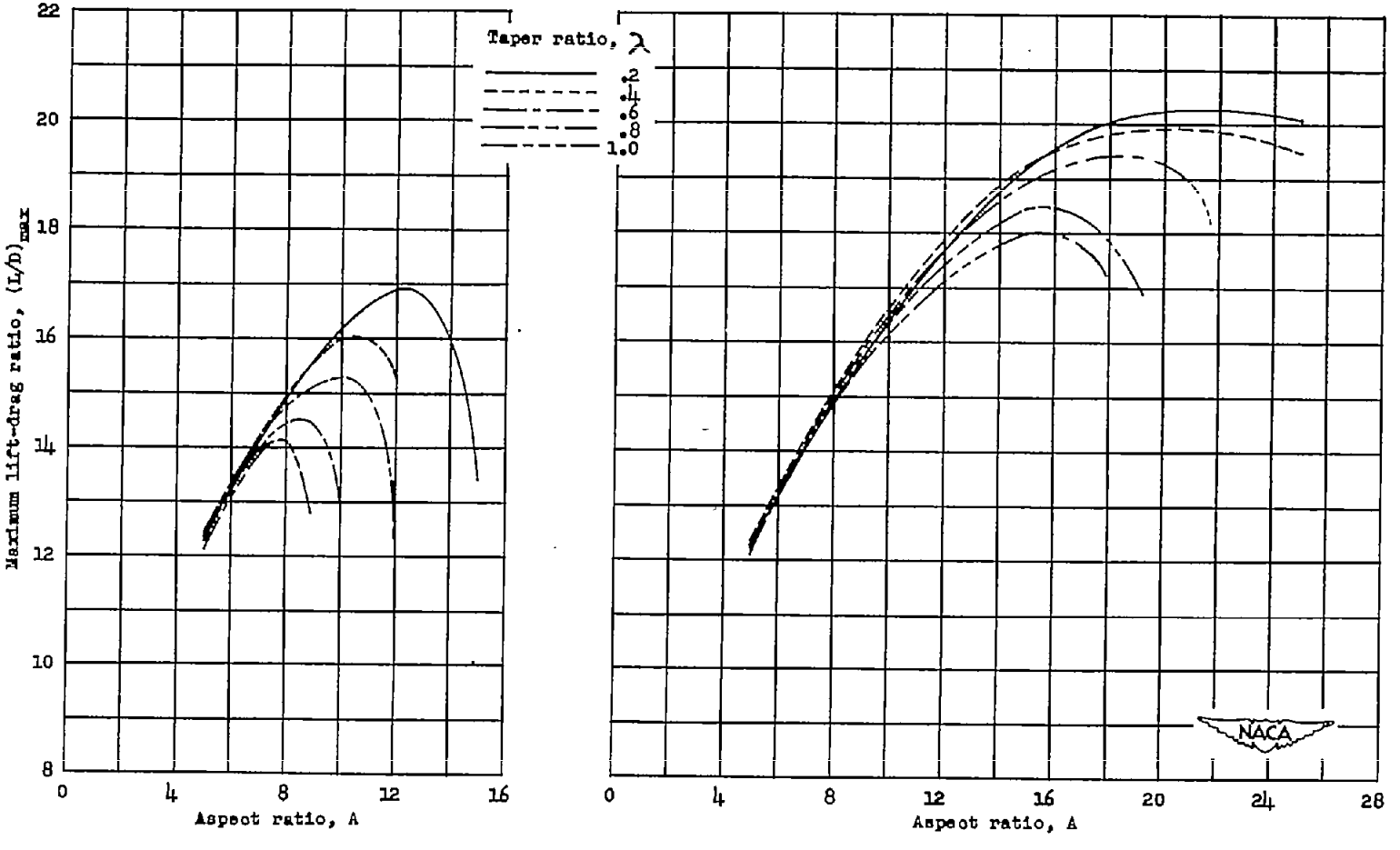

(a) Wing without boundary-layer control.

(b) Wing with boundary-layer control.

Figure 19.- Effect of aspect ratio on the maximum lift-drag ratio of a family of wings of various taper ratios with and without boundary-layer control and with a parasite-drag coefficient of 0.015 added.

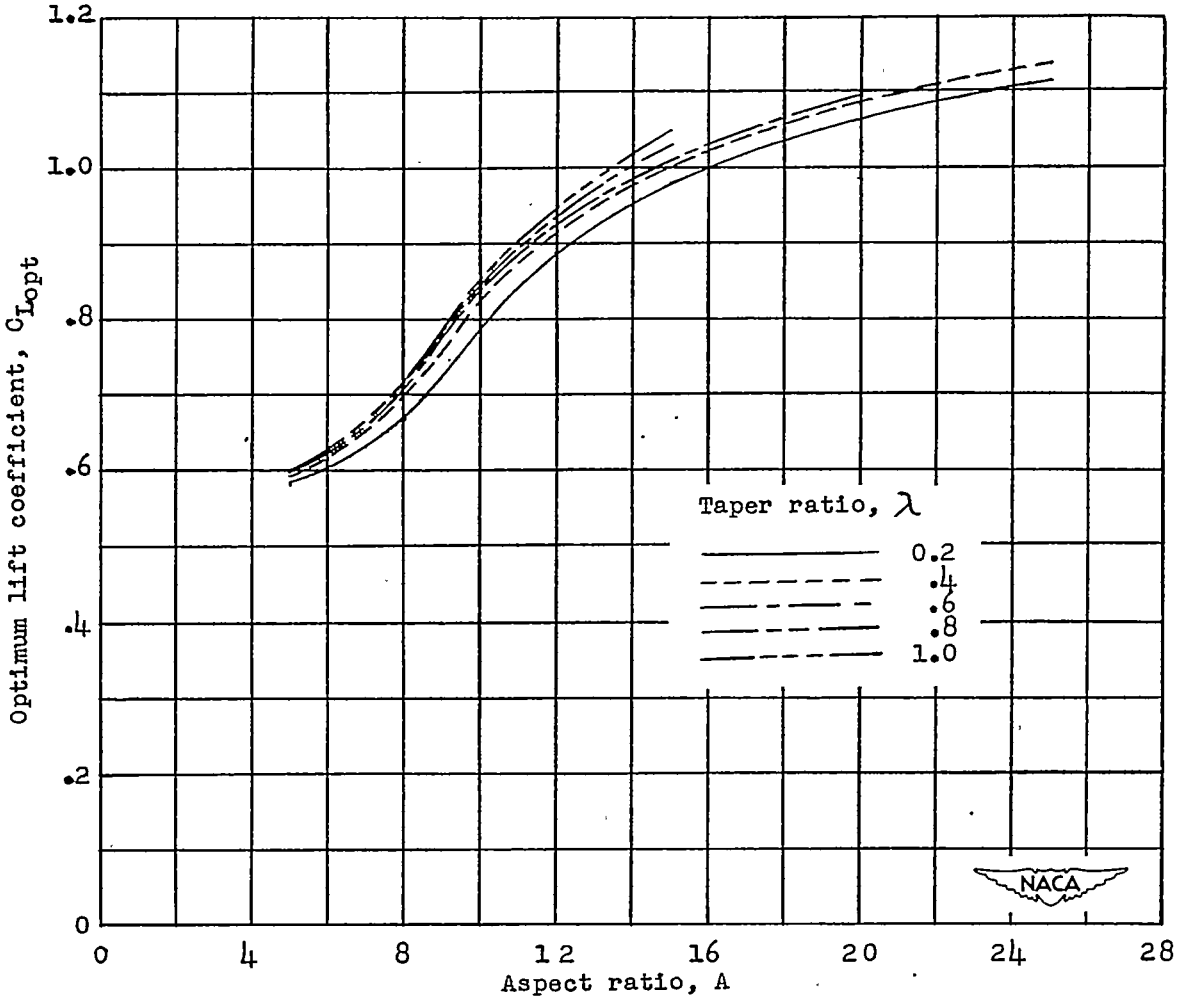

Figure 20.- Variation of optimum lift coefficient with aspect ratio for a family of wings of various taper ratios with boundary-layer control and with a parasite-drag coefficient of 0.015 added.

NACA-Langley - 7-16-51 - 1000